THERMAL MODELING & ANALYSIS OF CARBIDE TOOL USING FINITE ELEMENT METHOD

A Thesis

Submitted in partial fulfillment of the requirements for the award of degree

of

MASTER OF ENGINEERING

IN

CAD/CAM & ROBOTICS ENGINEERING

Submitted By

Amit Gupta

Roll No. 8038102

Under the supervision of

Mr.Gaurav Bartarya
Lecturer, MED
T.I.E.T., Patiala

Mr. Ravinder K Duvedi
Lecturer, MED
T.I.E.T., Patiala

MECHANICAL ENGINEERING DEPARTMENT
THAPAR INSTITUTE OF ENGINEERING AND TECHNOLOGY
(Deemed University)
PATIALA-147004, (INDIA)

June 2005

CERTIFICATE

This is to certify that the seminar entitled **" Thermal Modeling & Analysis of Carbide Tool Using Finite Element Method ",** being submitted by **Mr. Amit Gupta** in partial fulfillment of the requirements for the award of the degree of **Master of Engineering (CAD/CAM & Robotics Engineering) at Thapar Institute of Engineering and Technology (Deemed University), Patiala (INDIA)** is a bonafide work carried out by him under our guidance and supervision and that no part of this thesis has been submitted for the award of any other degree **.**

(Mr. Gaurav Bartarya)
Lecturer, MED
T.I.E.T. Patiala-147004(PUNJAB)

(Mr. Ravinder Kumar Duvedi)
Lecturer, MED
T.I.E.T. Patiala-147004(PUNJAB)

(Dr. S. K. Mohapatra)
Professor& Head, MED
T.I.E.T. Patiala-147004(PUNJAB)

(Dr. D. S Bawa)
Dean Academic Affairs
T.I.E.T. Patiala-147004(PUNJAB)

ACKNOWLEDGEMENT

I express my sincere gratitude to my guide, **Mr. Gaurav Bartarya**, and **Mr**. **Ravinder Kumar Duwedi**, **Mechanical Engineering Department**, **Thapar Institute of Engineering & Technology** for his valuable guidance, proper advice, and careful reviews of my work at all stages, and their highly appreciated instruction and constant encouragement during the course of my work on this thesis.

I am highly thankful to **Dr. Vijay Jadon, Asst. Prof., Mechanical Engineering Department, Thapar Institute of Engineering and Technology, Patiala** for his expert advice, technical suggestions and moral support during my thesis work.

Especially, I want to express my deepest appreciation and thanks to my supervisor **Mr. Sukhdev Chand** for his support and untiring help in conducting my experiments. I do not find enough words with which I can express my feeling of thanks to all my teachers and friends at T.I.E.T., for their help, inspiration and moral support which went a long way in completion of my thesis.

I am also thankful to the authors whose works I have consulted and quoted in this work. I also extend my thanks to all faculty and staff members of Mechanical Engineering Department, Thapar Institute of Engineering and Technology, for their direct and indirect help and cooperation.

(Amit Gupta)

ABSTRACT

The problem of tool wear monitoring in machining operations, has been an active area of research for quite a long time. The accurate prediction of tool wear is important to have a better product quality and dimensional accuracy. In cutting tools the area close to the tool tip is the most important region and conditions at the tool tip must be carefully examined, if improvements in tool performance are to be achieved

The present work involves the study of tool wear caused by the change in hardness of single point cutting tool for a turning operation to predict the tool life in orthogonal cutting based on the heat transfer analysis using Finite Element Method (FEM). The Experiments were performed with EN-24 steel as workpiece and Carbide uncoated tool bit as a tool material and the flank wear has been measured experimentally. An empirical relation is used to determine temperature at tool-tip and further Finite Element Method is used to determine the distribution of temperature over the surface of tool and its impact on hardness which is related by an empirical relations.

The study shows the effect of Modified temperature due to strain rate on carbide tool to describe the thermal softening of tool material and becomes prone to wear. The results reveal that by increasing process variables in machining the wear and temperature increases causing thermal softening of tool causing it to wear.

The results obtained have been verified with the available results from literature for the variation of wear with the temperature and thermal softening of carbide tool. The results prescribed demonstrate the significance of cutting parameters (speed, feed and depth of cut) in thermal analysis for study of the cutting tool wear.

INDEX

NOMENCLATURE

DIMENSIONAL PARAMETERS

X, Y, Z : Cartesian coordinate system

ξ, η : Local coordinates

Ω, Γ : Solution Domains

K : Conductivity coefficient

h : Convection coefficient

V : Cutting velocity

d : Depth of cut

f : Feed rate

ϕ : Shear Angle

α : Rake Angle

Q : Internal heat

$\dot{\gamma}$: Strain Rate

$\dot{\gamma}_o$: Reference Strain Rate

ν : Poisson's Ratio

MATRICES AND VECTORS

$[J]$: Jacobian matrix

$[N]$: Shape function matrix

$[K_c]$: Conductivity matrix

$[K_h]$: Convection matrix

$\{R_h\}$: Convection load vector

$\{R_q\}$: Heat flux load vector

$\{T\}$: Nodal pressure vector

LIST OF FIGURES

LIST OF TABLES

CHAPTER - 1
INTRODUCTION

Tool wear monitoring/sensing should be one of the primary objectives in order to produce the required end products in an automated industry so that a new tool may be introduced at the instant at which the existing tool has worn out, thus preventing any hazards occurring to the machine or deterioration of the surface finish. Cutting tools may fail due to the plastic deformation, mechanical breakage, cutting edge blunting, and tool brittle fracture or due to the rise in the interface temperatures.

Throughout the world today, there is a continuous struggle for cheaper production with better quality. This can be achieved only through optimal utilization of both material and human resources. Machining operations comprise a substantial portion of the world's manufacturing infrastructure. They create about 15% of the value of all mechanical components manufactured worldwide. Because of its great economic and technical importance, a large amount of research has been carried out in order to optimize cutting process in terms of improving quality, increasing productivity and lowering cost.

Tool wear influences cutting power, machining quality, tool life and machining cost. When tool wear reaches a certain value, increasing cutting force, vibration and cutting temperature cause surface integrity deteriorated and dimension error greater than tolerance. The life of the cutting tool comes to an end. Then the cutting tool must be replaced or ground and the cutting process is interrupted. The cost and time for tool replacement and adjusting machine tool increases cost and decreases the productivity. Hence tool wear relates to the economic of machining and prediction of tool wear is of great significance for the optimization of cutting process.

At present, the prediction of tool wear is performed by calculating tool life according to experiment and empirical tool life equations such as Taylor's equation or its extension versions. Although Taylor's equation gives the simple relationship between tool life and a certain cutting parameters, e.g. cutting speed, and is very easy to use, it gives only the information about tool life. For the researcher and tool manufacturer tool wear progress and tool wear profile are also concerned. Tool life equation gives no information about the wear mechanism. But capability of predicting the contributions of various wear mechanism is very helpful for the design of cutting tool material and geometry. In addition, such tool life equations are valid under very limited cutting conditions. For example, when tool geometry is changed, new equation must be established by making experiment.

Mostly researchers concentrate on the study of wear mechanism and investigate the mathematical relationship between wear due to various wear mechanisms and some cutting process variables such as relative sliding velocity of workpiece material along tool face, cutting temperature of tool face and normal pressure on tool face. Some tool wear equations related to one or several wear mechanisms are also developed, such as Usui's tool wear equation [15], and [19].

In the recent decades, with the emergency of more and more powerful computer and the development of numerical technique, numerical methods such as finite element method (FEM), finite difference method (FDM) and artificial Intelligence (AI) are widely used in machining industry. Among them, FEM has become a powerful tool in the simulation of cutting process because various variables in the cutting process such as cutting force, cutting temperature, strain, strain rate, stress, etc can be predicted by performing chip formation and heat transfer analysis in metal cutting, including those very difficult to detect by experimental method. Therefore a new tool wear prediction method may be developed by integrating FEM simulation of cutting process with tool wear model.

1.1 TOOL WEAR

Cutting tools are subjected to an extremely severe rubbing process. They are in metal-to-metal contact, between the chip and work piece, under conditions of very high stress at high temperature. The situation is further aggravated due to the existence of extreme stress and temperature gradients near the surface of the tool. During cutting, cutting tools remove the material from the component to achieve the required shape, dimension and finish. However, wears are occurring during the cutting action, and it will result in the failure of the cutting tool. When the tool wear reach certain extent, the tool or edge change has to be replaced to guarantee the ordinary cutting action.

1.1.1 TOOL WEAR PHENOMENA

Under high temperature, high pressure, high sliding velocity and mechanical or thermal shock in cutting area, cutting tool has normally complex wear appearance, which consists of some basic wear types such as crater wear, flank wear, thermal crack, brittle crack, fatigue crack, insert breakage, plastic deformation and build-up edge. The dominating basic wear types vary with the change of cutting conditions. Crater wear and flank wear shown in figure1.1 are the most common wear types [28].

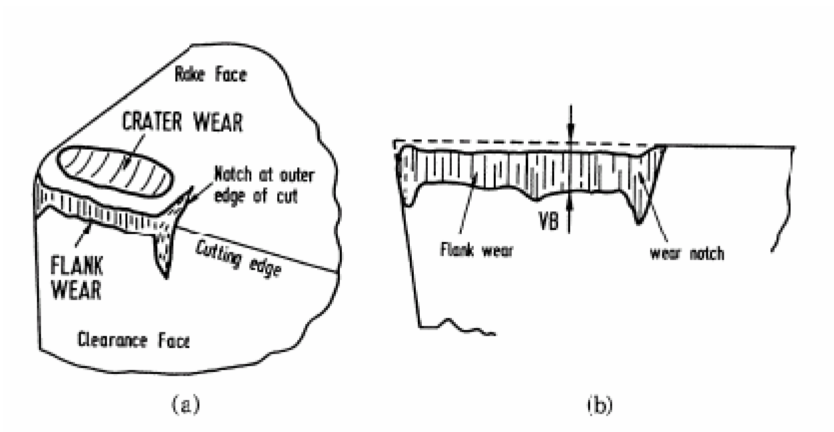

Figure1.1: Types of Tool Wear

- **Crater wear:** In continuous cutting, for example in turning operation, crater wear normally forms on rake face. It conforms to the shape of the chip underside and reaches the maximum depth at a distance away from the cutting edge where highest temperature occurs. At high cutting speed, crater wear is often the factor that determines the life of the cutting tool, because the tool edge is weakened by the severe cratering and eventually fractures. Crater wear is improved by selecting suitable cutting parameters and using coated tool or ultra-hard material tool. Crater wear and flank wear shown in figure1.1 are the most common wear types.

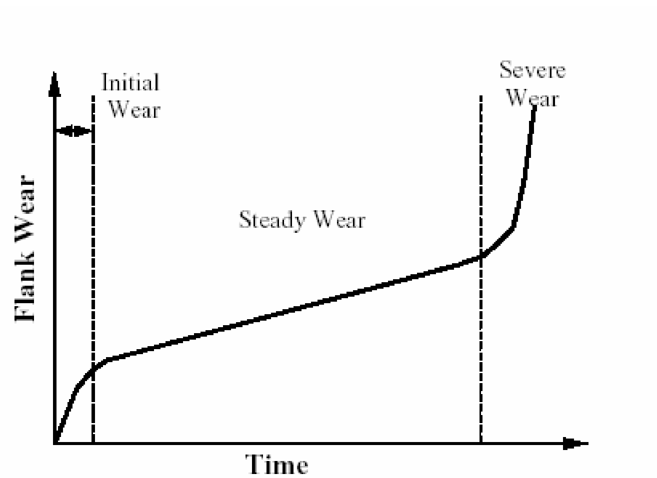

Figure 1.2: Behaviour of Flank wear

- **Flank wear:** Flank wear is caused by the friction between the newly machined work piece surface and the tool flank face. It is responsible for a poor surface finish, a decrease in the dimension accuracy of the tool and an increase in cutting force, temperature and vibration. Hence the width of the flank wear land “VB” is usually taken as a measure of the amount of wear and a threshold value of the width is defined as tool reshape criterion. Figure1.2 shows a variation of flank wear rate with cutting time, showing the initial wear, steady wear, and severe wear periods.

1.1.2 WEAR MECHANISM

In order to find out suitable way to slow down the wear process, many research works are carried out to analyze the wear mechanism in metal cutting. It is found that tool wear is not formed by a unique tool wear mechanism but a combination of several tool wear mechanisms.

Tool wear mechanisms in metal cutting include abrasive wear, adhesive wear, delamination wear, solution wear, diffusion wear, oxidation wear, electrochemical wear, etc. Among them, abrasive wear, adhesive wear, diffusion wear and oxidation wear are very important.

- **Abrasive wear:** Abrasive wear is mainly caused by the impurities within the workpiece material, such as carbon, nitride and oxide compounds, as well as the built-up fragments. This is a mechanical wear, and it is the main cause of the tool wear at low cutting speed.
- **Adhesive wear:** The simple mechanism of friction and wear proposed by Bowden and Tabor is based on the concept of the formation of welded junctions and subsequent destruction of these. Due to the high pressure and temperature, welding occurs between the fresh surface of the chip and rake face because of the chip flowing on the rake face results in chemically clean surface.

Severe wear is characterized by considerable welding and tearing of the softer rubbing surface at high wear rate, and the formation of relatively large wear particles. Adhesion wear occurs mainly at low machining temperatures on tool rake face, such built up edge (BUE).Under mild wear conditions, the surface finish of the sliding surfaces improves.

- **Diffusion wear:** Wear is a process of atomic transfer at contacting asperities. A number of workers have considered that the mechanism of tool wear must involve chemical action and diffusion. They have demonstrated welding and preferred chemical attack of (W) tungsten carbide in (W-Ti) tungsten-titanium carbides. There are several ways in which the wear may be dependent on the diffusion mechanism.

(i) Gross softening of the tool: Diffusion of carbon in a relatively deep surface layer of the tool may cause softening and subsequent plastic flow of the tool. This flow may produce major changes in the tool geometry, which result in high forces and a sudden complete failure of the tool.

(ii) Diffusion of major tool constituents into the work (Chemical element loss): The tool matrix or a major strengthening constituent may be dissolved into the work and chip surfaces as they pass the tool. In cast alloy, carbide or ceramic tools, this may be the prime wear phenomenon. With HSS tools, iron diffusion is possible, but it seems unlikely to be the predominant wear process. Diamond tool – cutting iron and steel is the typical example of diffusion wear.

(iii) Diffusion of a work-material component into the tool: A constituent of the work material diffusing into the tool may alter the physical properties of a surface layer of the tool. For example, the diffusion of lead into the tool may produce a thin brittle surface layer, this thin layer can be removed by fracture or chipping.

- **Oxidation wear:** High temperatures and the presence of air mean oxidation for most metals. A slight oxidation of tool face is helpful to reduce the tool wear. It reduces adhesion, diffusion and current by isolating the tool and the workpiece. But at high temperature soft oxide layers, for example Co_3O_4, WO3, TiO_2, are formed rapidly, and then taken away by the chip and the workpiece. This results in a rapid tool material loss, which is oxidation wear.
- **Chemical wear:** Corrosive wear (due to chemical attack of a surface)
- **Fatigue wear:** Fatigue wear is often a thermo-mechanical combination. Temperature fluctuations and the loading and unloading of cutting forces can lead to cutting edge cracking and breaking. Intermittent cutting action leads to continual generation of heat and cooling as well as shocks of cutting edge engagement.

Under different cutting conditions dominating wear mechanisms are different. For a certain combination of cutting tool and workpiece, the dominating wear mechanisms vary with cutting temperature, as shown in figure1.3. According to the temperature distribution on the tool face, it is assumed that crater wear is mainly caused by abrasive wear, diffusion wear and oxidation wear, but flank wear mainly dominated by abrasive wear due to hard second phase in the workpiece material.

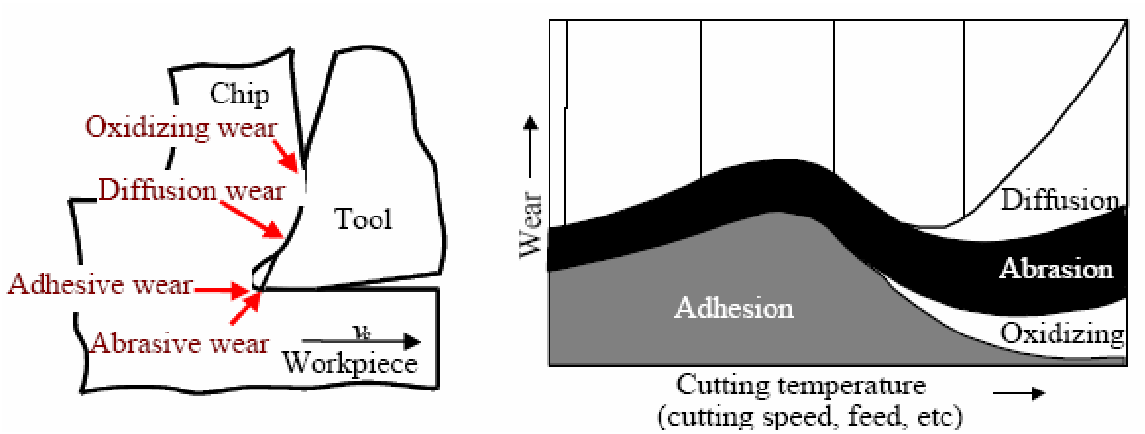

Figure 1.3: Wear mechanisms

1.1.3 PREDICTION OF TOOL WEAR

Prediction of tool wear is complex because of the complexity of machining system [15]. Tool wear in cutting process is produced by the contact and relative sliding between the cutting tool and the work piece and between the cutting tool and the chip under the extreme conditions of cutting area; temperature at the cutting edge can exceed 530°C and pressure is greater than 13.79 N/mm^2. Any element changing contact conditions in cutting area affects tool wear. Figure 1.4 shows influencing elements of the tool wear [15]. These elements come from the whole machining system comprising workpiece, tool, interface and machine tool:

- **Workpiece:** It includes the workpiece material and its physical properties (mechanical and thermal properties, microstructure, hardness, etc), which determine cutting force and energy for the applied cutting conditions.

Figure 1.4: Influencing elements of tool wear

- **Tool:** Tool material, tool coatings and tool geometric design (edge preparation, rake angle, etc) need to be appropriately chosen for different operations (roughing, semi-roughing, or finishing). The optimal performance of a cutting tool requires a right combination of the above tool parameters and cutting conditions (cutting speed, feed rate, depth of cut)
- **Interface:** It involves the interface conditions. In 80% of the industrial cutting applications, coolants are used to decrease cutting temperatures and likely reduce tool wear. Increasingly new technologies, such as the minimum liquid lubrication, have been developed to reduce the cost of coolant that makes up to 16% of the total machining costs.
- **Dynamic:** The dynamic characteristic of the machine tool, affected by the machine tool structure and all the components taking part in the cutting process, plays an important role for a successful cutting. Instable cutting processes with large vibrations (chatters) result in a fluctuating overload on the cutting tool and often lead to the premature failure of the cutting edge by tool chipping and excessive tool wear.

The problem of tool wear monitoring in machining operation has been active area of research. This is because tool change strategies, product quality, tooling costs, and productivity are all influenced by tool wear. Reduction in production cost and increase in productivity can be realized by making the most use of a tool's life and therefore increasing the time between tool changes.

1.1.4 TOOL WEAR MODELS

Many mathematical models are developed to describe tool wear in quantity. They can be categorized into two types: Tool life models and Tool wear rate models, and have been elaborated below.

Tool life models: This type of wear models gives the relationship between tool life and cutting parameters or variables. For example, Taylor's tool life equation reveals the exponential relationship between tool life and cutting speed, and Hastings tool life equation describes the great effect of cutting temperature on tool life [19], as shown in table 1.1. The constants n, C_1, A and B are defined by doing a lot of experiments with cutting speed changing and fitting the experimental data with the equation. It is very convenient to predict tool life by using this equation. In various sizes of cutting database, Taylor's tool life equation and its extension versions under different cutting conditions appear most frequently.

Tool life equations are suitable to very limited range of cutting conditions. As the new machining technologies, e.g. high-speed-cutting or dry cutting, are getting spread in manufacturing industry, the existing tool life equations need to be updated with new constants and a lot of experimental work has to be done. In addition, except that tool life can be predicted by these equations, it is difficult to get further information about the tool wear progress, tool wear profile or tool wear mechanisms that are sometimes important for tool designers.

Tool wear-rate models: These models are derived from one or several wear mechanisms. They provide the information about wear growth rate due to some wear mechanisms. In these modes, the wear growth rate, i.e. the rate of volume loss at the tool face (rake or flank) per unit contact area per unit time (mm/min), are related to several cutting process variables that have to be decided by experiment or using some methods.

Table 1.1: Tool life and Tool wear rate models

<table>
<tr><th>Empirical Tool Life Models</th><th>Tool Wear Rate Models</th></tr>
<tr><td>Taylor's basic equation:
$VL^n = C_1$ (n, C_1 = Constants)</td><td rowspan="2">Takeyama & Murata's wear model (considering abrasive wear and diffusive wear):
$$\frac{dW}{dt} = G(v, f) + D\exp\left(\frac{-E}{RT}\right)$$
(G,D =constants)</td></tr>
<tr><td>Taylor's extended equation:
$$L = \frac{C_2}{V^p f^q d^r}$$ (p,q,r,C_2 = constants)</td></tr>
<tr><td>Taylor's extended equation:
$$V = \frac{C_3}{L^m f^p d^q (BHN/200)^r}$$
(m,p,q,r,C_3 = constants)</td><td rowspan="2">Usui's wear model
(considering adhesive wear):
$$\frac{dW}{dt} = A\sigma_n V_s \exp\left(\frac{-B}{T}\right)$$
(A,B = Constants)</td></tr>
<tr><td>Temperature-based equation(known as Hasting's tool life equation):
$TL^B = A$
(A,B =constants)</td></tr>
<tr><td colspan="2">V = Cutting speed ,L = Tool life , σ_n = Normal Stress, f = Feed rate, d = Depth of cut
T = Cutting temperature ,BHN = Workpiece hardness, E = process activation energy
Vs = sliding velocity ,R = universal gas constant ,
dW/dt = wear rate (volume loss per unit contact area per unit time)</td></tr>
</table>

Takeyama & Murata's model is developed by considering the combination action of abrasive wear and diffusive wear. Therefore the equation sums two parts up. One part shows that abrasive wear is influenced by the cutting speed and feed. Another part including universal gas constant and tool temperature describes diffusive wear.

Usui's equation includes three variables: Sliding velocity between the chip and the cutting tool, tool temperature and normal pressure on tool face. These variables can be predicted by FEM simulation of cutting process or combining analytical method and FDM. Therefore Usui's equation is very practical for the implementation of tool wear estimation by using FEM or by using the combination of FDM and analytical method.

The constants in tool wear rate models are depending on the combination of workpiece and cutting tool material.

1.2 EFFECTS OF TOOL WEAR ON TECHNOLOGICAL PERFORMANCE

1.2.1 CONSEQUENCES OF TOOL WEAR

- Decrease the dimension accuracy;
- Increase the surface roughness;
- Increase the cutting force;
- Increase the temperature;
- Likely cause vibration;
- Lower the production efficiency, component quality;
- Increase the cost.

Influence on cutting forces: Flank wear (or wear-land formation) and chipping of the cutting edge affect the performance of the cutting tool in various ways. The cutting forces are normally increased by wear of the tool. Crater wear may, however, under certain circumstances, reduce forces by effectively increasing the rake angle of the tool. Clearance-face (flank or wear-land) wear and chipping almost invariably increase the cutting forces due to increased rubbing forces.

Surface finish (roughness): The surface finish produced in a machining operation usually deteriorates as the tool wears. This is particularly true of a tool worn by chipping and generally the case for a tool with flank-land wear – although there are circumstances in which a wear land may burnish (polish) the workpiece and produces a good finish.

Dimension accuracy: Flank wear influences the plan geometry of a tool this may affect the dimensions of the component produced in a machine with set cutting tool position or it may influence the shape of the components produced in an operation utilizing a form tool.

Vibration or chatter: The vibration is another aspect of the cutting process which may be influenced by flank wear. A wear land increases the tendency of a tool to dynamic instability. A cutting operation which is quite free of vibration when the tool is sharp may be subjected to an unacceptable chatter mode when the tool wears.

1.2.2 CHARACTERISTICS OF TOOL WEAR

- Huge contact stress at the rake and flank surface
- High temperature (800-1000 °C for carbide and steel combination)

Hence, generalized wear theory cannot be directly used for accurate study of the tool wear.

1.3 THERMAL ANALYSIS:

In machining operations, mechanical work is converted to heat through the plastic deformation involved in chip formation and through friction between the tool and workpiece. Some of this heat conducts into cutting tool, resulting in high tool temperatures near cutting edge. Elevated tool temperatures have negative impact on a tool life. The temperature of the tool plays an important role in the thermal distortion and the, machined part's dimensional accuracy, as well as in the tool life in machining. Tools become softer and wear more rapidly by abrasion as temperatures are increased, and in many cases constituents of the tool life may diffuse into the chip or react chemically with the workpiece or cutting fluid.

1.3.1 HEAT GENERATION IN MACHINING

Heat generation while machining has significant influence on machining. It can increases tool wear and thereby reducing tool life [17]. It gives rise to thermal softening of cutting tool. It is commonly accepted that both the wear and failure mechanisms which develop in cutting tools are predominantly influenced by temperature and it also results in modification to the properties of workpiece and tool material such as hardness. In order to predict the wear and failure characteristics of a tool, it is necessary to quantify the temperatures which develop during the cutting operation.

In machining operations, mechanical work is converted to heat through the plastic deformation involved in chip formation and through friction between the tool and workpiece. Figure 1.5 shows three regions of heat generation in turning; which are, the shear zone, the chip-tool interface and the tool-workpiece interface zone [17]:

- **The shear zone:** The shear zone, where the main plastic deformation takes place due to shear energy. This heat raises the temperature of the chip. Part of this heat is carried away by the chip when it moves upward along the tool. Considering a continuous type chip, as the cutting speed increases for a given rate of feed, the chip thickness decreases and less shear energy is required for chip deformation so the chip is heated less from this deformation. About 80-85% of the heat generated in shear zone.
- **The chip-tool interface zone**: The chip-tool interface zone, where secondary plastic deformation due to friction between the heated chip and tool takes place. This causes a further rise in the temperature of the chip. This chip-tool interface contributes 15-20% of heat generated.

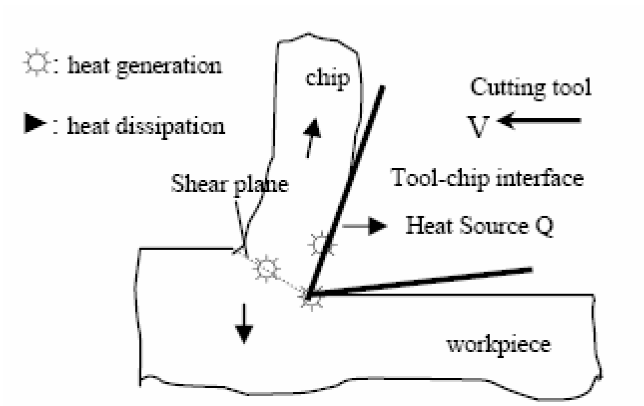

Figure 1.5: Zones of heat generation & dissipation during the metal cutting process.

- **The tool-workpiece interface zone:** The work-tool interface zone 3, at flanks where frictional rubbing occurs. This area contributes 1-3% of heat generated.

As the portion of heat that flows into the tool cause very high temperature in vicinity of tool tip which in turn decrease the hardness of the tool material and in extreme case may even cause melting. The wear rate of tool therefore increases, resulting in a decrease in useful life of the tool. It is increasingly important to understand how machining temperature are affected by the process variable involved which are cutting speed, feed rate, and tool geometry.

1.3.2 ANALYSIS TECHNIQUES

Several methods have been used for measuring the temperatures generated during metal cutting operations [12]. The main techniques used to evaluate the temperature during machining are as following:

Experiment Retrospection: Many experimental methods have been devised to measure the tool, chip or workpiece temperature and their distribution, these are:

- Tool-Chip Thermocouple Technique
- Embedded Thermocouple Technique
- Infrared Radiation Technique
- Metal Microstructure and Micro-hardness Variation Measurement
- Thermo-sensitive Painting Technique
- Temper Color Technique

Numerical Simulation: The numerical methods were successfully applied in calculating the temperature distribution and thermal deformation in tool, chip and workpiece. Especially, the finite element and boundary element methods can deal with very complicated geometry in machining; they have great potential to solve the problems in practice. These numerical methods used in measurement of temperatures are the following:

- Finite Difference Method
- Finite Element Method
- Boundary Element Method

Semi-Analysis: In the semi analysis technique, some information such as chip surface temperature or temperature distribution in workpiece is first obtained experimentally. Then the temperature distribution and/or thermal deformation in chip and sometimes in the tool and workpiece as well are calculated analytically. The inverse heat transfer problem in machining is an example of these methods.

1.3.3 HEAT TRANSFER IN MACHINING

Heat is transferred across boundaries by conduction, convection and radiation because of the temperature gradient, and air present at ambient temperature [8].

- Heat transfer inside the chip and workpiece, the tool and tool-holder is by conduction.
- Heat transfer between coolant/air and the chip/tool/workpiece is by convection.
- Radiation is rarely investigated in traditional machining operations.

1.3.4 HEAT EFFECTS

In metal cutting, severe deformations take place in the vicinity of the cutting edge of the tool because of the high temperatures resulting from machining operation. These elevated temperatures have a negative impact on tool life, and quality of surface. Following are some of the effects of heat on various cutting parameters:

- Heat Influences on Cutting Forces: The heat influence on the cutting forces is mainly because of the following reasons-the friction co-efficient is tightly dependent upon temperature, and the properties of cut material also depend on temperature.
- Heat Effects on Tool Life
- Heat Influences on Surface Toughness
- Heat Influences on Thermal Deformation in Lathe.
- Heat Effects on Mass Transfer in Coolant Circulation System.

1.3.5 Finite Element Method in Thermal Analysis

Finite element analysis is a most useful and accurate approach for the determination of field variables that is made possible by advancements in computational and processing power of computers and thus it is almost used for all the computer aided design methodologies in recent years. Applications range from deformation and stress analysis to field analysis of heat flux, fluid flow, magnetic flux, seepage and other flow problem. In this method of analysis, a complex region defining a continuum is discredited into simple geometric shapes called finite elements. The Present work is also based on the application of finite element for thermal analysis of single point cutting tool for turning operation. Once the model developed for determination of temperature field for single point cutting tool, it can also be implemented for other multipoint processes like drilling, milling or grinding also.

CHAPTER - 2
LITERATURE REVIEW

The problem of tool wear monitoring in machining operations has been an active area of research for quite some time. The machining processes are inherently dynamic in nature due to various factors. Some of them can be mathematically modeled, but others are too uncertain. Thus simplifications are made while modeling the extremely complex machining processes. Research in the field of machining has been primarily done on single point turning process, as it is the basic metal removal processes. Once a model has been developed for turning operation, it can be implemented for other multipoint processes like drilling, milling or grinding.

In this work tool wear along with temperature had been selected as the criterion for the process control in turning operation. In recent years, numerical calculating methods have been widely developed in most areas of engineering and have been used to determine the thermal behaviour of cutting tools. In general, the application of finite element and finite difference techniques has been successful, yet still relies heavily on the accuracy of experimentally determined boundary conditions.

This chapter deals with the review of the work done on the topic. Firstly the review is on the general analysis of tool, concentrating mainly on prediction of temperature and tool wear. Then the concentration shifts on to second part, which is the review on use of finite element in the thermal analysis of the cutting tool.

2.1 MODELS FOR DETERMINATION OF TEMPERATURE FIELD

Temperature measurement and prediction have been a major focus of machining research for several decades. Throughout the 20^{th} century, much effort has been undertaken into measuring the temperature generated during cutting operations. Interfacial temperatures in machining play a major role in tool wear and can also result in modification to the mechanical properties of the workpiece and cutting tool.

Leshock et al [4] presented the results the tool chip interface temperature measurement by the tool work thermocouple technique. Tool chip interface temperature is analyzed under a wide range of cutting condition during turning of 4140 steel alloys and Inconel 718 nickel based alloys with tungsten carbide tools. The obtained experimental results are compared with the predictions based on the Loewen and Shaw's model. In addition an empirical model for the tool face temperature terms of cutting parameters is established. Finally, the tool chip interface temperature is analyzed with both flank and crater wear during machining of 4140 steel alloys.

Sullivan et al [12] presented different methods used for the measurement of temperature of a single cutting tool. Initial experiments conducted involved the simultaneous measurement of forces & temperature. Use of the tool-chip interface as a thermocouple was one of the first methods of estimating interfacial temperatures in machining process. These experiments focused on the use of embedded thermocouples and using the infrared camera to monitor the process.

Komanduri et al [13] addresses two fundamental thermal issues of tribology in orthogonal machining with a sharp tool, namely, the nature of the apparent heat partition in the shear plane and the variable heat partition at the chip-tool interface. The distribution of temperature in the chip, the tool, and the work material was determined analytically considering the combined effect of these two heat sources in orthogonal machining. The new analytical model was verified for a wide range of Peclet numbers, using the available experimental data from the literature.

Huda et al [14] developed a technique for measuring temperature at the interface between a cutting tool and a chip. A two-color pyrometer with fused fiber coupler was applied to the temperature measurement of the tool-chip interface in dry and wet turning. By using this pyrometer, it is possible to measure the temperature of a very small object without emissivity affecting the results. The temperature distributions on the cutting tool and the work material were analyzed using the finite element method. Good agreement was obtained between the analytical results and experimental ones.

Miller et al [21] developed Experimental techniques using modern, digital infrared imaging and successfully applied them during this study to gather cutting tool temperature distributions from orthogonal machining operations. This new process has seemingly overcome many problems associated with past experimental techniques.

Ranc et al [23] developed a high-speed broad band visible pyrometer using an intensified CCD camera (spectral range: 0.4 mm–0.9 mm) for the measurement of the machining temperature. The maximum temperature in the chip can reach 730°C and minimal temperature which can be detected is around 550°C. The advantage of the visible pyrometry technique is to limit the temperature error due to the uncertainties on the emissivity value and to have a good spatial resolution (3.6 mm) and a large observation area.

2.2 APPLICATION OF FEM FOR TOOL WEAR RESEARCH

A more promising approach for developing an orthogonal metal cutting model is provided by an advanced numerical discretization scheme, such as the finite element method. This part basically discusses about the application of FEM in predicting the tool temperature and thus estimating the tool wear.

Shih et al [1] developed the, methodology using FEM for the simulation of plane–strain orthogonal cutting processes with continuous chip formation. The orthogonal metal cutting experiment was setup on a shaper, and the distributions of the residual stresses of the annealed carbon steel are measured using the X-ray diffraction method. Along with this, they also developed experimental procedures for orthogonal metal cutting and measurement of distributions of residual stresses using the X-ray diffraction method. They formulated a 4 nodes 8 degree of freedom, quadrilateral plane–strain finite element. The finite element formulation was divided in two phases. Only thermal finite element formulation is discussed here.

- **Thermal finite element formulation:** The temperature increment during the metal cutting process is simulated using a linear thermal finite element formulation by assuming that the thermal conductivity, density and heat capacity of the workpiece material remain unchanged during the displacement increment. The thermal finite element formulation for temperature analysis can be written in a matrix form as

$$[C]\left\{\dot{T}\right\} + \left([K_k] + [K_c]\right)\{T\} = \left\{\dot{F}p\right\} + \left\{\dot{F}t\right\} \tag{2.1}$$

Where, $[C] = \int_v \{N\}\{N\}^T \rho c dV$

$[K_k] = \int_v [B]^T [B] k dV$

$[K_c] = \int_{S_c} \{N\}^T \{N\} h dS_c$

$$\{\dot{F}_p\} = \int_v \{N\}\dot{q}\,dV$$

Here, {T} = Temperature vector at nodal points

{N} = Shape function vector

c = Heat capacity of workpiece

h = Convection coefficient

S_c = Convection boundary of the workpiece

$\{\dot{F}_p\}$ = Vector of heat generation due to plastic work

$\dot{q}$ = Rate of plastic work

$\{\dot{F}_t\}$ = Heat generation rate on the boundary node of the workpiece due to frictional work

ρ, c, k , and h are all assumed as direction independent.

Based on the equation (2.1), the temperature distribution of the workpiece is obtained and the material properties are thus generated.

Shih [2] developed plane – strain Finite Element Method and applied to analyze the orthogonal metal cutting process. Detailed work-material modeling, which included the coupling of large strain, high strain rate and temperature effects, was used to simulate the material deformation during cutting process. The finite element predictions of the residual stresses were compared with measurements obtained from X-ray diffraction. They concluded that finer element mesh configuration should be used to achieve more accurate modeling of the cutting process and also to improve the FE predictions.

Gillibrand et al [3] developed a technique to predict the temperatures generated along the tool/chip interface using standard analytical methods. The temperature distribution along the tool/chip interface is applied as a heat source input to a finite element model of the tool. They developed a package for estimating the thermal behavior of both single and multi-point cutting tools using base data which are generally available, or may be acquired through standard cutting tests. They concluded that with the continued development of surface engineered cutting tools, and the product testing involved, this easy-to-apply, rapid, low-cost package would be useful for giving an indication of the expected thermal behavior of surface engineered cutting tools.

Mills et al [5] developed a technique to monitor the deformation and crack propagation around inclusions using a micro cutting device in a scanning electron microscope while machining is being carried out. The temperature distribution field within a cutting tool under conditions of adherent layer formation was determined using the FEM. It was found that the temperature gradient in the cutting tool from the tool face at a position 0.25 to 0.5 mm from the major cutting edge is much smaller in the presence of an adherent layer than without an adherent layer.

Tieu et al [6] presented a research work carried out on the cutting tool temperature field with adhering layer formation when machining Ca-S tree-cutting stainless steel. By means of combining thermocouple measuring method and finite element (FE) analysis, the cutting temperature distributions and their relation with the formation of adhering layer were investigated. Based on the experimental work using a miniature thermocouple and the analytical results from FE modeling, they concluded that the adhering layer thickness was uneven and the average temperature of cutting zone for adhering layer formation was within a range of 950-1050°C.

Chu et al [7] developed technique for measuring temperature close to primary cutting edge in turning operation. The cutting temperatures of a 0.16 % carbon bright drawn mild steel, have been measured for a range of cutting speed and feedrates at a constant depth of cut. Tool nose radius was also varied. The correlations for workpiece temperature of cutting speed & feed have been developed. It showed that cutting speed & feed rates have significant impact on temperature but nose radius has little effect.

Ostafiev et al [8] analyzed heat flux transfer in the cutting tool in steady state orthogonal cutting. The method involved as interactive procedure to determine temperature distributions in the tool from varying heat flux transfer conditions. The temperature distributions determined from this procedure were compared with those obtained experimentally. A coincidence of the experimental and theoretical temperature distributions implied that the chosen heat flux model was appropriate.

Yen et al [15] developed a methodology to estimate the tool wear of carbide tool in orthogonal cutting using FEM. In metal cutting, tool wear is strongly influenced by the cutting temperature, contact stresses, and relative sliding velocity at the interface. These process variables depend on tool and workpiece materials, cutting condition, tool geometry, use of coolants etc, for the given application. Based on temperatures and stresses on the tool face, tool wear may be estimated with acceptable accuracy by using an empirical wear model and using FEM simulation. The methodology proposed by them has three different phases, the first phase includes, a development of tool wear model for the specified tool-workpiece pair, the second phase includes, modifications in the commercial FEM code and last phase includes experimental validation of the developed methodology. The wear prediction procedure starts with a coupled thermo-viscoplastic Lagrangian cutting simulation with isotropic strain-hardening using DEFORM®-2D. In order to obtain the cut chip geometry near the steady state, a special simulation module, "Konti-Cut", developed by WZL at University of Aachen (RWTH), Germany, was utilized.

Zhao et al [18] developed a methodology to investigate the effects of the internal cooling on the flank wear of the cutting tools in orthogonal cutting. A flank wear model for a cutting tool in orthogonal cutting is presented which is based on previous wear models and includes the normal stress and the effect of temperature on the flank wear. According to the prediction of this model, the wear performance of carbide cutting tools and HSS cutting tools are different due to their different thermal softening behavior, and they have formulated the following methodologies:

1. Flank wear model for orthogonal metal cutting

In all the previous wear models studied by them, hardness H and normal stress σ_t are two main parameters closely related to the wear and the wear rate is usually proportional to σ_t and inversely proportional to H. Mathematically wear can be expressed as follows:

$$dW = K\frac{\sigma_t dL}{H}$$

The wear volume can be converted to the wear land measurement VB with the assumption of a zero degree rake angle of the cutting tool

$$W = \frac{1}{2} w V_B^2 \tan\theta$$

Where, W is the volume worn away on the relief face, V_B is the measurement of wear land on the tool, w the width of cut and θ is the relief angle of the tool[18], as shown in figure 2.1. The apparent area of the tool–work contact interface can be written as follows: $A = w\,V_B$

The normal stress at the flank face can be calculated as given by the following relation:

$$\sigma_t = \frac{F_t}{A} = \frac{F_t}{wV_B}$$

Where F_t is the thrust force in cutting .V_B is a variable that increases with the development of flank wear. Thus the equation to predict flank wear can be written as:

$$V_B = K\left(\frac{2V_c}{w^2 \tan\theta}\right)^{\frac{1}{3}}\left(\frac{F_t t}{H}\right)^{\frac{1}{3}}$$

Where, K is a coefficient which can be determined by experiments, *L* is the cutting length, H is the hardness of the cutting tool, V_C is the cutting speed, and t is the cutting time.

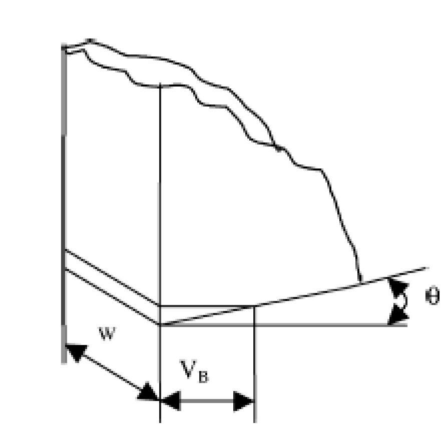

Figure 2.1: Schematic of cutting tool with zero degree rake angle, where w is the tool width, V_B the flank wear and θ is the relief angle

2. Effects of temperature on flank wear in orthogonal cutting

To consider the effects of the temperature on the flank wear, it is necessary to know the thermal softening of the cutting tool material versus the temperature. The exponential function used to predict thermal softening is as follows:

$$H(T) = H_o \exp(-\alpha T)$$

Where H (*T*) is the hardness of a material at a given temperature, *T* is in °C, H_o and α are constants obtained by Curve-fitting .Since the relationship between the thermal softening and temperature can be obtained by curve-fitting experimental data, different equations can be used. The following is the equation used them:

$$H(T) = C_1T^3 + C_2T^2 + C_3T + C_4$$

Where H is the hardness of the cutting tool material, T is the temperature in ˚C and C_1, C_2, C_3 and C_4 are constants that can be determined by curve-fitting. The values of C_1, C_2, C_3 and C_4 for different tool materials are:

For Carbide Tool Material

$C_1 = 0.000006$, $C_2 = -0.0054$, $C3 = 0.5853$, and $C_4 = 1517$.

For HSS Tool Material

$C_1 = -0.000002$, $C_2 = 0.0002$, $C_3 = -0.2122$, and $C_4 = 853.81$.

The flank wear in arbitrary units versus the temperature was calculated by them for both carbide and HSS material.

YC Yen et al [19] developed a methodology to estimate the tool wear and tool life of a carbide tool in orthogonal cutting using FEM simulation. The proposed procedure for predicting the tool wear at any time instance t_k was divided in four phases.

- "Konti Cut" Simulation
- Pure Heat Transfer Analysis
- Calculating Tool Wear Rate
- Updating the Tool Geometry

The simulations using a cutting tool with constantly updated rake face and flank face geometries have shown that it is possible to predict the evolution of tool wear at any given cutting time from FEM simulations by using the proposed methodology by them.

Amir et al [20] developed methodology to extend the applicability of Oxley's analysis of machining to a broader class of materials beyond the carbon steels used by Oxley and co-workers. The performance of the model was studied by comparing its predictions with experimental data for different materials and it was found that model accurately produces the dependence of the cutting forces and chip thickness as a function of undeformed chip thickness and cutting speed and accurately estimates the temperature in the primary and secondary shear zones.

Arsecularatne et al [22] investigated the application of the Oxley modeling approach to high speed machining (HSM) process for gaining a fundamental understanding and performance prediction of this process which is gaining increased popularity due to its many economic and technological advantages such as faster metal removal rates, efficient use of machine tools and, improved surface finish and lower cutting forces. In the present work, this theory has been applied for two plain carbon steels and low alloy steel under HSM conditions. The predicted cutting forces, chip thicknesses, and secondary deformation zone thicknesses are then compared with the experimental results obtained under identical conditions. Good agreement has been shown between measured and predicted results.

Moufki et al [26] developed an analytical approach for thermomechanical modeling of oblique cutting process. The material characteristics such as strain rate sensitivity, strain hardening and thermal softening were considered. A critical study was also presented by them in order to show the influences of the input parameters of the model including the normal shear angle, the thickness of the primary shear zone and the pressure distribution at the tool–chip interface. The model permits to predict the cutting forces, the chip flow direction, the contact length between the chip and the tool and the temperature distribution at the tool–chip interface which has an important effect on tool wear.

Molinari et al [27] developed an analytical approach to model the thermomechanical process of chip formation in a turning operation. The model presented can be used to predict the cutting forces, the global chip flow direction, the surface contact between chip and tool and the temperature distribution at the rake face which affects strongly the tool wear. The tendencies predicted by the model were also compared qualitatively with the experimental trends founded in the literature.

2.3 SUMMARY OF LITERATURE

From above literature review, it can be concluded that FEM has been effectively implemented to determine the temperature distribution on the tool surface, in order to predict the tool wear. Since machining parameters affect the wear and heat generation in tool, so further study has been carried out to develop the relation between machining parameters and mechanical properties which are governed by modified machining temperatures due to strain rate.

CHPATER - 3
INSTRUMENTATION AND EXPERIMENTATION

The objective of the present work is to develop methodology to relate tool wear with mechanical properties of a material such as Hardness. Here hardness is related with the modified temperature, including the effect of strain rate, of cutting tool. Finite Element Analysis is used to depict the temperature at various points of cutting tool by changing various machining parameters such as cutting speed (V), depth of cut (d), feed rate (f).

3.1 INSTRUMENTATION

The various instruments used for experimentation are discussed here in this section:

3.1.1 FORCE MEASUREMENT

A force measurement actually involves the measurement of a deflection, caused by that force, with a suitable calibration between the force and the deflection it produces. For measuring small deflections, various devices have been used. Some of them are listed below:

1. The dial indicator.
2. Pneumatic devices.
3. Optical devices.
4. Piezoelectric crystals.
5. Strain Gauges.

Out of these, most widely used dynamometer is of strain gauge type. In this category, bounded- wire strain gauges have commonly been used. Usually these bonded wire gauges have been specified by the resistance and the gauge factor (F). The gauge factor is a measure of sensitivity of gauge and is defined as:

$$F = \frac{\Delta R/R}{\Delta l/l} = \frac{\Delta R}{\in R}$$

Where, $\in$ is the normal strain and can be calculated as: $\in = \frac{\Delta l}{l}$

In our case, bonded wire strain gauge of resistance 120+ and gauge factor 2, have been used. In order to measure the strains of the order of 1+, the changes of the resistance of the same order of magnitude need to be measured. This can be made by means of Wheatstone bridge as shown in figure 3.1[24]. No current will flow through the galvanometer (G) if the four resistances satisfy the equation

$$\frac{R_1}{R_4} = \frac{R_2}{R_3}$$

For the sake of simplicity, the lathe operation is frequently taken as a orthogonal cutting process. In this case, the resultant force will act in a known plane and only two force components are required to analyze the cutting process. A schematic diagram of the dynamometer used in the present work is shown in the figure 3.2[24]. In the present case, the axial cutting force, *Fc,* and the tangential cutting force, *Ff,* have been used.

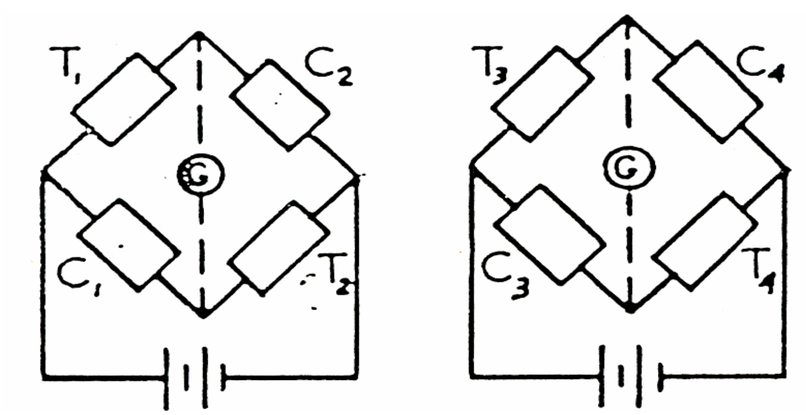

Figure 3.1: Wheatstone bridge

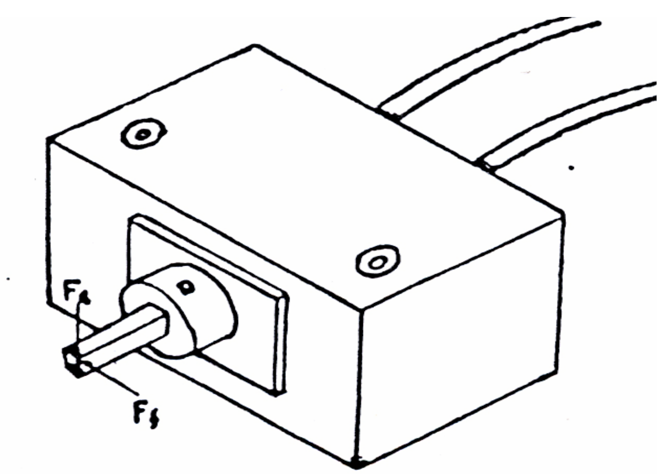

Figure 3.2: Dynamometer

A two component cutting force dynamometer of cantilever type is used in the present work. The dynamometer structure is made of aluminum. The action of the forces is to bend the structure. The axial cutting force*, Fc,* bends the structure about the one axis and the tangential feed force, *Ff,* bends the structure about another axis. Strain gauges have been used to measure these distortions (moments), and the recordings are calibrated to give a measure of the forces applied.

3.2 EXPERIMENTATION

Experiments were carried out on a turning lathe. A carbide tip turning tool was clamped in a two component strain gauge dynamometer using a tool holder designed in a machine lab during the thesis work. For the experimentation, EN 24 steel workpiece of 600mm length was held in a three – jaw chuck and supported by a center in the tail stock. Tool height and tool overhang was set to the required level with the help of gauges. A rough turning pass was made initially to eliminate the runout of the workpiece. The output flank wear was measured with the help of a tool room microscope. The straight edge with Rake angle $\alpha = 0$ has been used to have an orthogonal cutting.

3.2.1 PLANNING OF EXPERIMENT

A scientific approach to planning of experiments must be incorporated in order to perform an experiment most effectively. Statistical design of experiments is the process of planning the experiments so that the appropriate data could be collected which may be analyzed by statistical method resulting in valid and objective conclusions.

Planning of experiments was employed in order to fulfill the following requirements:

- To get the data uniformity distributed over the whole range of controllable factors to be investigated.
- To reduce the total number of experiments.
- To establish a relationship between different input variables and the output accurately in the selected range of investigation

3.2.2 EXPERIMENTAL PROCEDURE

The experiments were made on the HMT lathe using a bar turning process under dry conditions. For the range of range of cutting conditions (cutting speed, feed, and depth of cut) it was required to measure the two force components F_t and F_f, thickness of chip and flank wear. A total of eight experiments were carried out, all with the same basic configuration and carbide inserts were replaced after performing a single test so as to see the effect of temperature on the tool individually at different cutting conditions. The selected ranges of each parameter used are given below:

- **Work material:** The EN 24 Steel (0.35- 0.45 %C, 0.45- 0.6 %Mn, 1.3 - 1.8 %Ni) was chosen for the present investigation with a diameter of 60 mm and 600 mm length.

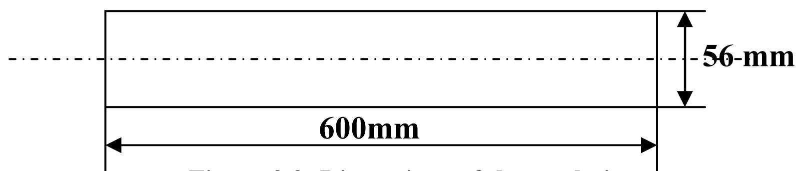

Figure 3.3: Dimensions of the workpiece

The figure 3.3 shows the dimensions of the workpiece (EN24) before the turning process.

- **Tool material:** The tool material used should be capable of high speed machining with dry cutting conditions. In present investigation carbide inserts were used for performing the experiments.
- **Tool geometries:**

a) Tool length: 16.02mm
b) Tool width: 8.02 mm
c) Nose radius: 0.4 mm

- **Test conditions:** carbide inserts were used to machine EN24 steel with following cutting parameters

a) Rotational speed:70.08 – 179.82 (m/min)
b) Feed: 0.0787 – 0.175 (m/sec)
c) Depth of cut: 0.508,0.762,1.27 (mm)

3.2.3 EXPERIMENT METHODOLOGY

A HMT make lathe was used for turning experiment whose specifications have been given in appendix -A. Figure3.4 shows the schematic diagram of the machine and equipment setup.

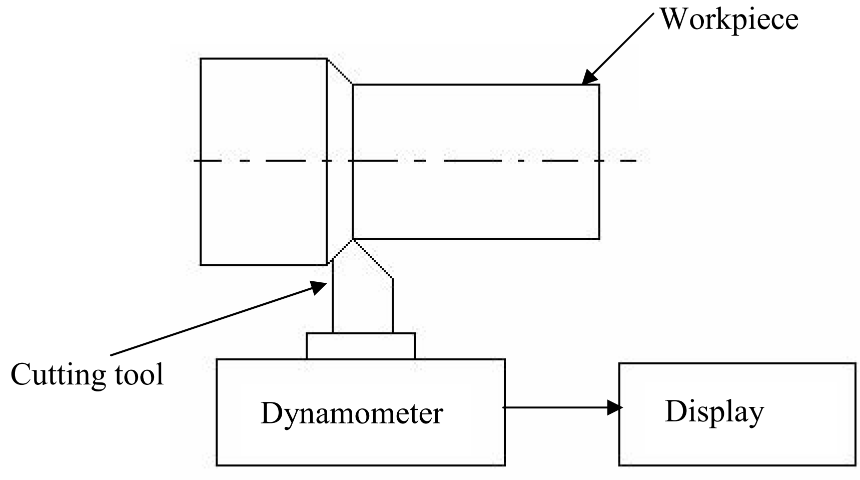

Figure 3.4: Schematic diagram of the lathe and equipment setup

Then the actual experiments have been carried out with the different input cutting conditions for different experiments for constant volume of material removal in each case. The experiments carried out can be classified**:**

1. Carry out experiment on lathe machine using EN 24 as work piece and commercial available Carbide Tool of triangular shape.
2. Machining is done with different sets of Cutting speed, depth of cut, & feed rates.
3. Measuring the cutting forces with dynamometer.
4. Measuring the deformed chip thickness using vernier calliper.
5. Measuring the flank wear of the carbide insert with microscope.
6. Correlating these wear trend with thermal softening of tool due to rise in temperature in insert.

The output flank wear is measured with the help of a metallurgical microscope having graduation marked on the eyepiece. These input cutting conditions are fed to program and value of temperature and Hardness at every nodes of the tool is thus calculated.

CHAPTER - 4
ANALYSIS

The present chapter deals with the formulation of three-dimensional governing equation for heat conduction used to obtain the temperature distribution on the face of the tool bit, to be used for obtaining the hardness at the various positions on the tool. The eight noded brick elements have been used for the FEM modeling.

4.1 GOVERNING EQUATION FOR THE HEAT TRANSFER

Governing equation for the heat transfer problem can be written as:

$$\frac{\partial}{\partial x}\left(K\frac{\partial T}{\partial x}\right)+\frac{\partial}{\partial y}\left(K\frac{\partial T}{\partial y}\right)+\frac{\partial}{\partial z}\left(K\frac{\partial T}{\partial z}\right)+Q=0 \quad (4.1)$$

Following assumptions have been considered for the simplicity if the computation required:

1. Conduction occurs in the steady state,
2. Material is isotropic and homogeneous as ($K_x = K_y = K_z = K$)
3. Internal heat generation is zero.

This equation is solved with appropriate boundary conditions, and heat transfer is considered in three-dimensional solid Ω bounded by a surface Γ .

4.2 BOUNDARY CONDITION

Following boundary conditions have been used for the solution of the present problem:

1. Temperature is specified at nodes which are in touch with shear zone[1], [4], [20],and [22], and have been calculated by relation given below:

$$T_{mod}\ (^{o}K) = T_{avg}\left(1-\nu\log\frac{\dot{\gamma}}{\dot{\gamma}_o}\right)$$

$$\text{Here, } \dot{\gamma} = \frac{\cos\ \alpha}{\cos\ (\phi - \alpha)} \cdot \frac{V}{\Delta y}$$

$$\phi = \tan^{-1}\left(\frac{r\ \cos\ \alpha}{1-r\ \sin\alpha}\right)$$

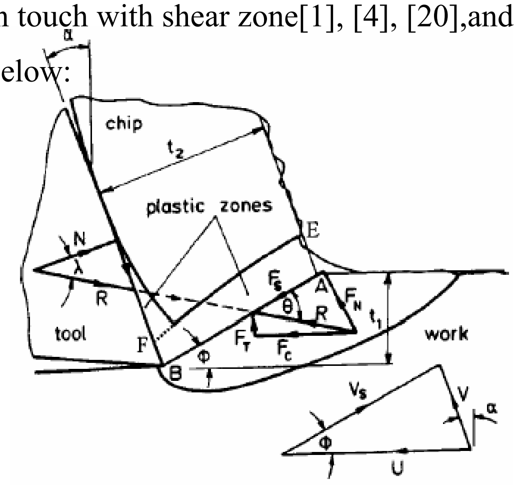

Figure 4.1: Model of chip formation used in Oxley's analysis for Orth. machining

Δy = spacing between successive planes (25 *10^{-4} mm)

$$T_{avg.interface}(^{o}C) = 1700V^{0.5}d^{0.2}f^{0.4}$$

2. Convection is taking place on surface from the tool bit to air, taking

Where, $T_{\infty} = 27\ ^{o}C$

$q_n = h(T - T_{\infty})$

h_{air} =14 W/m^2 ^{o}C

q_n = Heat flux normal to the boundary

T_{∞} = Ambient temperature

4.3 FEM FORMULATION

Using Galerkin's orthogonality, equation (4.1) becomes;

$$\int_{\Omega}\left(\frac{\partial}{\partial x}\left(K\frac{\partial T}{\partial x}\right)+\frac{\partial}{\partial y}\left(K\frac{\partial T}{\partial y}\right)+\frac{\partial}{\partial z}\left(K\frac{\partial T}{\partial z}\right)\right)N_i d\Omega + \int_{\Omega} QN_i d\Omega = 0 \qquad (4.2)$$

Where $d\Omega = dx.dy.dz$

Now, since internal heat generation has been assumed to be zero;

Thus, $\int_{\Omega} QN_i d\Omega = 0$

The various components of equation (4.2) can be obtained from the relations as written below:

$$\int_{\Omega}\frac{\partial}{\partial x}\left(K\frac{\partial T}{\partial x}\right)N_i d\Omega = \int_{y,z} N_i K\frac{\partial T}{\partial x}dy.dz - \int_{\Omega} K\frac{\partial T}{\partial x}\frac{\partial N_i}{\partial x}dx.dy.dz$$

$$= \int_{\Gamma} N_i K\frac{\partial T}{\partial x}d\Gamma - \int_{\Omega} K\frac{\partial T}{\partial x}\frac{\partial N_i}{\partial x}d\Omega$$

$$\int_{\Omega}\frac{\partial}{\partial y}\left(K\frac{\partial T}{\partial y}\right)N_i d\Omega = \int_{x,z} N_i K\frac{\partial T}{\partial y}dx.dz - \int_{\Omega} K\frac{\partial T}{\partial y}\frac{\partial N_i}{\partial y}dx.dy.dz$$

$$= \int_{\Gamma} N_i K\frac{\partial T}{\partial y}d\Gamma - \int_{\Omega} K\frac{\partial T}{\partial y}\frac{\partial N_i}{\partial y}d\Omega$$

$$\int_{\Omega}\frac{\partial}{\partial z}\left(K\frac{\partial T}{\partial z}\right)N_i d\Omega = \int_{x,z} N_i K\frac{\partial T}{\partial z}dx.dy - \int_{\Omega} K\frac{\partial T}{\partial z}\frac{\partial N_i}{\partial z}dx.dy.dz$$

$$= \int_{\Gamma} N_i K \frac{\partial T}{\partial z} d\Gamma - \int_{\Omega} K \frac{\partial T}{\partial z}\frac{\partial N_i}{\partial z} d\Omega$$

Thus, the equation (4.2) becomes;

$$\int_{\Gamma} N_i K \frac{\partial T}{\partial x} d\Gamma + \int_{\Gamma} N_i K \frac{\partial T}{\partial y} d\Gamma + \int_{\Gamma} N_i K \frac{\partial T}{\partial z} d\Gamma - \int_{\Omega} K\left(\frac{\partial T}{\partial x}\frac{\partial N_i}{\partial x} + \frac{\partial T}{\partial y}\frac{\partial N_i}{\partial y} + \frac{\partial T}{\partial z}\frac{\partial N_i}{\partial z}\right) d\Omega = 0 \tag{4.3}$$

Let q_x, q_y, and q_z be the heat flux in x, y and z direction respectively and can be written as:

$q_x = -K\frac{\partial T}{\partial x}$, $q_y = -K\frac{\partial T}{\partial y}$ and $q_z = -K\frac{\partial T}{\partial z}$

Putting these values of q_x, q_y, q_z in equation (4.3), we have:

$$-\int_{\Gamma} N_i\left(q_x n_x + q_y n_y + q_z n_z\right) d\Gamma - \int_{\Omega} K\left(\frac{\partial T}{\partial x}\frac{\partial N_i}{\partial x} + \frac{\partial T}{\partial y}\frac{\partial N_i}{\partial y} + \frac{\partial T}{\partial z}\frac{\partial N_i}{\partial z}\right) d\Omega = 0 \tag{4.4}$$

Where, n_x, n_y, n_z are the direction cosines of unit normal to the surfaces.

And, let $q_n = q_x n_x + q_y n_y + q_z n_z$

Therefore equation (4.4) becomes,

$$-\int_{\Omega} N_i q_n d\Gamma - \int_{\Omega} K\left(\left(\frac{\partial T}{\partial x}\frac{\partial N_i}{\partial x}\right) + \left(\frac{\partial T}{\partial y}\frac{\partial N_i}{\partial y}\right) + \left(\frac{\partial T}{\partial z}\frac{\partial N_i}{\partial z}\right)\right) d\Omega = 0 \tag{4.5}$$

Here, q_n is normal heat along the unit outward normal, which is specified by boundary conditions.

Now the heat flux in the tool is because of the heat load at the specified contact of tool and workpiece, and heat loss because of convection at the other surfaces of the tool exposed to air/coolant.

Thus, $\int N_i(q_n) d\Gamma = \int q_o N_i d\Gamma + \int N_i\left(h\left(T - T_\infty\right)\right) d\Gamma$ (4.6)

From equations (4.5) and equation (4.6), the final FEM equation has been developed, as written below:

$$-\underbrace{\int_{\Gamma} q_o N_i \, d\Gamma}_{1} - \underbrace{\int_{\Gamma} N_i h\left(T - T_\infty\right) d\Gamma}_{2} - \int \underbrace{K\left[\frac{\partial N_i}{\partial x}\ \frac{\partial N_i}{\partial y}\ \frac{\partial N_i}{\partial z}\right]}_{3}\begin{bmatrix}\frac{\partial T}{\partial x}\\ \frac{\partial T}{\partial y}\\ \frac{\partial T}{\partial z}\end{bmatrix} d\Omega = 0 \qquad (4.7)$$

Explanation of each part of above equation (4.7) is as given below:

1. The first part of equation (4.7) is represented $\{R_q\}$,which represents heat load vector arising from specified surface heating

$$\{R_q\} = -\int_{\Gamma} q_o [N]^T \, d\Gamma$$

$$[N]^T = \begin{bmatrix} N_1 \\ N_2 \\ N_3 \\ N_4 \end{bmatrix}$$

Where, N_i =, N_1, N_2, N_3, N_4, are shape functions

Γ Represents surface area A

Further, vector $\{R_q\}$ can also be written as

$$\{R_q\} = \int_{-1}^{+1}\int_{-1}^{+1} q_o \ [N]^T \ dA$$

Here, dA=|det J| $d\xi d\eta$

Where

$$N_1 = \left(1 - \eta - \xi + \eta\xi\right)/4$$

$$N_2 = \left(1 - \eta + \xi + \eta\xi\right)/4$$

$$N_3 = \left(1 + \eta + \xi - \eta\xi\right)/4$$

$$N_4 = \left(1 + \eta - \xi - \eta\xi\right)/4$$

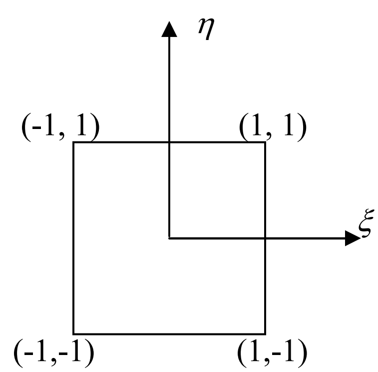

Jocobian matrix also represented as [J], which can be expanded as given below

$$[J]=\begin{bmatrix} \frac{\partial N_1}{\partial \xi}x_1+....+\frac{\partial N_8}{\partial \xi}x_8 & \frac{\partial N_1}{\partial \xi}y_1+...+\frac{\partial N_8}{\partial \xi}y_8 & \frac{\partial N_1}{\partial \xi}z_1+...+\frac{\partial N_8}{\partial \xi}z_8 \\ \frac{\partial N_1}{\partial \eta}x_1+...+\frac{\partial N_8}{\partial \eta}x_8 & \frac{\partial N_1}{\partial \eta}y_1+...+\frac{\partial N_8}{\partial \eta}y_8 & \frac{\partial N_1}{\partial \eta}z_1+...+\frac{\partial N_8}{\partial \eta}z_8 \\ \frac{\partial N_1}{\partial \zeta}x_1+...+\frac{\partial N_8}{\partial \zeta}x_8 & \frac{\partial N_1}{\partial \zeta}y_1+...+\frac{\partial N_8}{\partial \zeta}y_8 & \frac{\partial N_1}{\partial \zeta}z_1+...+\frac{\partial N_8}{\partial \zeta}z_8 \end{bmatrix}$$

Finally {Rq} equation written as below,

$$\{R_q\}=\int_{-1}^{1}\int_{-1}^{1} q_o[N]^T\,[J]\ d\xi\ d\eta \tag{4.8}$$

2. Second part of the equation (4.7) can be further expressed in two separate parts as written below:

$$-\int_{\Gamma} N_i h(T-T_\infty)d\Gamma=-\int_{\Gamma} N_i hTd\Gamma+\int_{\Gamma} N_i hT_\infty d\Gamma$$

Where, h = convective heat transfer coefficient

T_∞ = convective exchange temperature of air/fluid.

T = unknown surface temperature.

The first part of above equation is heat load vector arising from surface convention and denoted as $\{R_h\}$

$$\{R_h\}=\int_{\Gamma} N_i\ h\ T_\infty\ d\Gamma \tag{4.9}$$

Now vector $\{R_h\}$ can further be written as:

$$\{R_h\}=\int_{-1}^{1}\int_{-1}^{1}[N]^T\ h\ T_\infty\ |J|\ d\xi\ d\eta$$

Second part represents element conduction matrix related to convention and represented as:

$$[k_h]\{T\} = -\int_{\Gamma} N_i \ h \ T \ d\Gamma$$

Here, $[K_h]$ = Element Conductance Matrix related to Convection,

$\{T\}$ = Element Nodal Temperature Vector.

Where, $T = \sum_{i=0}^{8} N_i T_i$

Or, $T = N_1T_1 + N_2T_2 + \ldots\ldots\ldots\ldots\ldots\ldots + N_8T_8$

Putting this in above equation,

Thus we have, $$[K_h] = \int_{-1}^{1}\int_{-1}^{1} h[N]^T [N] \ |J| \ d\xi \ d\eta \tag{4.10}$$

3. The third part of equation (4.7) is the element conductance matrix related to the conduction (coefficient matrix). It is represented by $[K_c] \ \{T\}$

Where, $$[K_c]\{T\} = \int_{\Omega} K \begin{bmatrix} \frac{\partial N_i}{\partial x} & \frac{\partial N_i}{\partial y} & \frac{\partial N_i}{\partial z} \end{bmatrix} \begin{bmatrix} \frac{\partial T}{\partial x} \\ \frac{\partial T}{\partial y} \\ \frac{\partial T}{\partial z} \end{bmatrix} d\Omega \tag{4.11}$$

Temperature gradient within the element is given by

$$\frac{\partial T}{\partial x} = \frac{\partial N_1}{\partial x} T_1 + \frac{\partial N_2}{\partial x} T_2 + \frac{\partial N_3}{\partial x} T_3 \ldots\ldots\ldots\ldots\ldots\ldots + \frac{\partial N_8}{\partial x} T_8 \tag{4.11a}$$

$$\frac{\partial T}{\partial y} = \frac{\partial N_1}{\partial y} T_1 + \frac{\partial N_2}{\partial y} T_2 + \frac{\partial N_3}{\partial y} T_3 \ldots\ldots\ldots\ldots\ldots\ldots + \frac{\partial N_8}{\partial y} T_8 \tag{4.11b}$$

$$\frac{\partial T}{\partial z} = \frac{\partial N_1}{\partial z} T_1 + \frac{\partial N_2}{\partial z} T_2 + \frac{\partial N_3}{\partial z} T_3 \ldots\ldots\ldots\ldots\ldots\ldots + \frac{\partial N_8}{\partial z} T_8 \tag{4.11c}$$

In matrix form, the above relations can be represented as:

$$\begin{bmatrix} \frac{\partial T}{\partial x} \\ \frac{\partial T}{\partial y} \\ \frac{\partial T}{\partial z} \end{bmatrix} = \begin{bmatrix} \frac{\partial N_1}{\partial x} & \frac{\partial N_2}{\partial x} & \cdots\cdots & \frac{\partial N_8}{\partial x} \\ \frac{\partial N_1}{\partial y} & \frac{\partial N_2}{\partial y} & \cdots\cdots & \frac{\partial N_8}{\partial y} \\ \frac{\partial N_1}{\partial z} & \frac{\partial N_2}{\partial z} & \cdots\cdots & \frac{\partial N_8}{\partial z} \end{bmatrix}_{3\times 8} \begin{bmatrix} T_1 \\ T_2 \\ T_3 \\ T_4 \\ T_5 \\ T_6 \\ T_7 \\ T_8 \end{bmatrix}_{8\times 1}$$

Using the above relations equation (4.11) can be written as

$$[K_c] = \int_{-1}^{1}\int_{-1}^{1}\int_{-1}^{1} K \; B^T B \; |J| \; d\xi \; d\eta \; d\zeta \tag{4.12}$$

Where B matrix is given as

$$B = \begin{bmatrix} \frac{\partial N_1}{\partial x} & \frac{\partial N_2}{\partial x} & \cdots & \cdots & \frac{\partial N_8}{\partial x} \\ \frac{\partial N_1}{\partial y} & \frac{\partial N_2}{\partial y} & \cdots & \cdots & \frac{\partial N_8}{\partial y} \\ \frac{\partial N_1}{\partial z} & \frac{\partial N_2}{\partial z} & \cdots & \cdots & \frac{\partial N_8}{\partial z} \end{bmatrix}$$

B^T is the transpose of B matrix.

To achieve the close boundary representation the scientists have developed curvilinear side element based on transforming simple geometric shapes of some local coordinate system into distorted shapes in global Cartesian system and then evaluating the element equation for the distorted element. The parent element may be selected from lagrangian / serendipity family. The Local Coordinate System associated with parent element is called curvilinear coordinate.

The Serendipity coordinates for elements are represented as:

$$x = \sum_{i=1}^{n_c} M_i \; x_i$$

$$y = \sum_{i=1}^{n_c} M_i \ y_i$$

$$z = \sum_{i=1}^{n_c} M_i \ z_i$$

Here, n_c = Total number of nodes per element

and for isoparametric elements, $M_i = N_i$

Therefore, $x = \sum_{i=1}^{8} N_i \ x_i$

$$y = \sum_{i=1}^{8} N_i \ y_i$$

$$z = \sum_{i=1}^{8} N_i \ z_i$$

Here, N_i is a function of (ξ ,η ,ζ).

Now to evaluate the B–matrix we need to evaluate the derivative of shape function with respect to x, y and z. The derivative cannot be found out directly as shape function is expressed in terms of natural coordinates (ξ ,η ,ζ). So by using chain rule differentiation

$$\frac{\partial N_i}{\partial \xi} = \frac{\partial N_i}{\partial x} \cdot \frac{\partial x}{\partial \xi} + \frac{\partial N_i}{\partial y} \cdot \frac{\partial y}{\partial \xi} + \frac{\partial N_i}{\partial z} \cdot \frac{\partial z}{\partial \xi}$$

$$\frac{\partial N_i}{\partial \eta} = \frac{\partial N_i}{\partial x} \cdot \frac{\partial x}{\partial \eta} + \frac{\partial N_i}{\partial y} \cdot \frac{\partial y}{\partial \eta} + \frac{\partial N_i}{\partial z} \cdot \frac{\partial z}{\partial \eta}$$

$$\frac{\partial N_i}{\partial \zeta} = \frac{\partial N_i}{\partial x} \cdot \frac{\partial x}{\partial \zeta} + \frac{\partial N_i}{\partial y} \cdot \frac{\partial y}{\partial \zeta} + \frac{\partial N_i}{\partial z} \cdot \frac{\partial z}{\partial \zeta}$$

$$\begin{bmatrix} \frac{\partial N_i}{\partial \xi} \\ \frac{\partial N_i}{\partial \eta} \\ \frac{\partial N_i}{\partial \zeta} \end{bmatrix} = \begin{bmatrix} \frac{\partial x}{\partial \xi} & \frac{\partial y}{\partial \xi} & \frac{\partial z}{\partial \xi} \\ \frac{\partial x}{\partial \eta} & \frac{\partial y}{\partial \eta} & \frac{\partial z}{\partial \eta} \\ \frac{\partial x}{\partial \zeta} & \frac{\partial y}{\partial \zeta} & \frac{\partial z}{\partial \zeta} \end{bmatrix} \begin{bmatrix} \frac{\partial N_i}{\partial x} \\ \frac{\partial N_i}{\partial y} \\ \frac{\partial N_i}{\partial z} \end{bmatrix}$$

The final heat transfer equation can be written as

$$\left[[K_c] + [K_h] \right] \{T\} = \{R_h\}$$

The above equation can be further written in the form as given below

$$[K]\{T\} = \{Q\} \tag{4.13}$$

Where

[K] = Thermal conductance coefficients matrix

{T}= Nodal temperature vector.

{Q}= Nodal heat flux or heat load vector.

4.4 HARDNESS OF TOOL

Since effects of temperature are being considered on flank wear, so it becomes necessary to consider thermal softening of cutting tool material. Relationship between temperature and thermal softening can be given by [18]

$$H(T) = C_1T^3 + C_2T^2 + C_3T + C_4$$

Where H is hardness of cutting tool material, T is temperature in ^{o}C and C_1, C_2, C_3, and C_4 are constants for tool material.

For carbides tool the values for these are:

C_1 = 0.000006, C2 = -0.0054, C_3 = 0.5853, C4=1517

4.5 SOLUTION SCHEME

- The three-dimensional solution domain corresponding to tool bit is discredited for the solution of the final heat conduction equation (4.13) and appropriate boundary conditions are applied.
- The value of elemental matrices [Kc] and [Kh] are calculated in functions **stiff( )** and **convection_stiff( )** and they are added appropriately to find L.H.S. of the equation 4.10 and 4.12 respectively.
- The [Rh] matrix is calculated as per equation in **function load( )**
- Appropriate boundary condition are applied in **boundary( )** and then the global {T} vector is calculated from function **solver( ).**
- The function **separate( )** gives the values of {T}, which are thus used in function **hardness( )** to calculate the value of hardness at different nodes.

4.6 FLOW CHART OF SOLUTION PROCEDURE

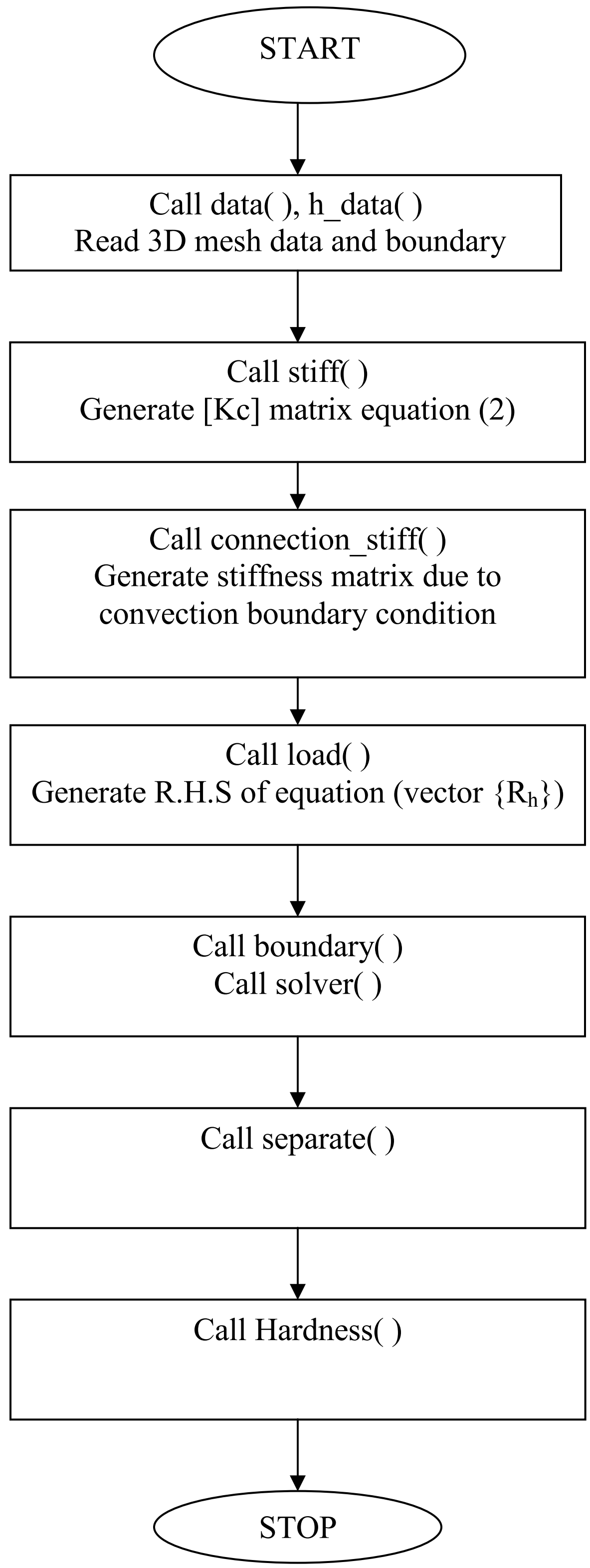

CHAPTER - 5
RESULTS AND DISCUSSIONS

In the present chapter the results for the present problem, that is for the solution of the thermal softening of the tool material in order to predict the tool wear have been developed in accordance with the previously developed models for tool wear [4], [20] and [22]. The number of experiments has been conducted to find out the cutting forces and flank wear of the tool, made of tungsten carbide, at varying machining parameters, which are cutting speed (V), cutting feed (f) and depth of cut (d). Using the experimental data, the strain rate and average interface temperature for the various cutting conditions have been obtained, which have been ultimately used to determine the modified temperature at the tool and the workpiece contact area. The measured experimental values are than fed into the FEM program to predict the temperature at all the nodes of a cutting tool. For simplicity the tool is assumed to be a single point with zero nose radius. This temperature of contact area have been used to determine the overall temperatures at the various parts of the cutting tool using the heat transfer equation developed and using the FEM methods for the solution of these equations for the present problem with the appropriate boundary condition as has been explained in chapter 4. This predicted temperature is than related with the hardness of the cutting tool (Thermal softening).

5.1 MACHINING PARAMETERS USED FOR EXPERIMENTATION

Table 5.1: Cutting parameters

Cutting speed v (rpm) (Range)	Feed f (mm/rev) (Range)	Depth of cut d (mm) (Range)
420	0.08	0.5
710	0.16	0.75

The table 5.1 shows the numerical values of the various machining parameters (cutting speed, feed and the depth of cut), that have been selected for experimentation, for the measurement of the temperature, strain rate and flank wear. The EN24 steel workpiece material has been used for experimentation, and its specifications have been shown in appendix B. The cutting material used is Tungsten Carbide, and its specification has been mentioned in appendix C.

The table 5.2 shows the experimental values of wear, strain-rate and resultant cutting forces for different speed, feed and depth of cuts for the different set of experiments conducted on the carbide cutting tool. The levels of the process variables, which have been used for the experiments of the validation set, are in between the [-1, 1] range. Here, -1 stands for the minimum, and +1 stands for the maximum level of parameters.

Table 5.2: Experimental Results of measured parameters against parameters V, f and d

S. No.	v	d	f	Wear(exp)in mm	Strain Rate(exp) $1s^{-1}$	Resultant Forces (N)
1	-1	-1	-1	0.02	577	340
2	-1	-1	+1	0.025	569	410
3	-1	+1	-1	0.03	165	470
4	-1	+1	+1	0.035	550	560
5	+1	-1	-1	0.045	840	245
6	+1	-1	+1	0.05	880	500
7	+1	+1	-1	0.065	820	390
8	+1	+1	+1	0.075	830	398

To eliminate the effect of wear on the experiments, the tools have been replaced after every cut of constant volume of workpiece material. In total eight carbide bits have been used for all the different set of experiments to be conducted. Tool edge has been made straight or parallel to the chuck to have an orthogonal cut. Constant volume signifies that equal amount of material was removed in all the different sets of experiment conducted. This has been done so that all the measurements should be taken correctly at the same operating conditions to have a good accuracy in results with minimum possible error.

The relationship between machining parameters and temperature generated at tool workpiece interface has been calculated using the empirical relations as mentioned in the references [4], [24], and [26]. The temperature at tool tip was calculated by changing different depth of cut, feed rate and cutting velocity. Strain rate has also been measured using the empirical relations and than both the measured temperature and the strain rate are put into the equation to find the modified temperature which considers the effect of both.

This temperature has been applied to analyze the temperature distribution on the tool at different edge, nodes and elements through finite element analysis, considering heat loss because of conduction in the tool material and convection with air at ambient temperature. Tool material hardness has been calculated with the help of the temperature distribution obtained as a result of FEM analysis [18]. The results have been obtained for tool wear with the change in machining parameters by relating the heat generated at the tool-workpiece interface and taking hardness of tool material as a function of temperature [18].

5.2 MODELLING OF SOLUTION DOMAIN USING FEM

In order to use the finite element technique, mathematical expressions have been derived and discussed in the previous chapter and have been used to predict the temperature at the various locations of the cutting tool. Computer program in VC^{++} environment based on the FEM formulation presented in the previous chapter have been developed and numerical results for temperature and its effect on the hardness of the cutting tool have been obtained and discussed in preceding topics.

The following are the details of the discritization of the solution domain carried out for the FEM Analysis and thus used in the developed computer program for the generation of the results.

Problem is for	: 3 D heat conduction
Type of elements	: Eight Noded brick elements (Serendipity family)
Total node	: 288
Total element	: 168
Node per element	: 8
Node per face	: 4
Number of fixed nodes	: 3 (temperature at the tip of the cutting tool)
Number of convection Faces	: 6 (shown in Appendix–C)

The properties of the cutting tool used (Carbide bits) are:

$\nu = 0.18$, $\dot{\gamma} = 1\ s^{-1}$, T_{∞} =27°C (for air), K = 0.076 W/m^{2}k

5.3 VALIDATION OF RESULTS

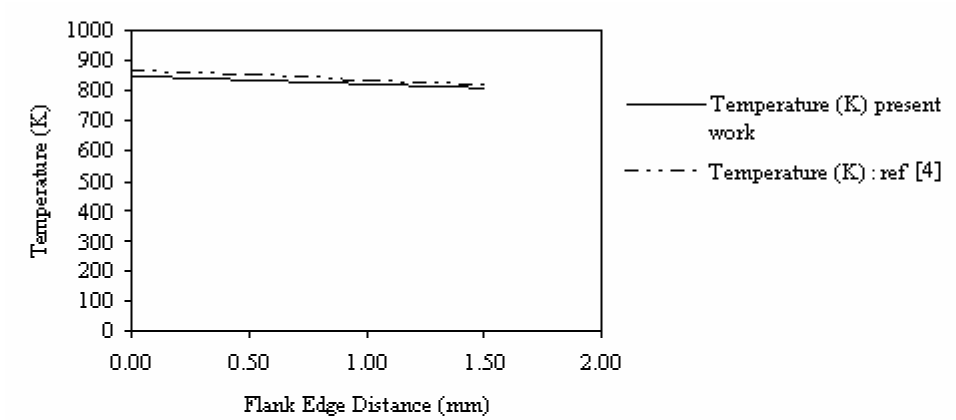

Figure 5.1: Relationship between Cutting tool temperature and flank distance

In order to check the validity of the analysis and the solution procedure discussed in chapter 4, the results for temperature field and its effect on thermal softening of cutting tool have been obtained from the developed computer program by using the experimental data of strain-rate and flank wear, and have been compared with the results of Leshock et al [4], for checking the validity of the results. The relation between flank edge distance and the final temperature variation on the cutting tool have been developed for the range of the cutting parameters as given in the table 5.1, and have been shown here in graphically form in figure 5.1. It is interpretable from the graph, that as we move away from the flank edge, the temperature keeps on decreasing and thus the tip of the carbide cutting tool is prone to more wear rather than the distances away from the tool tip. The results from the reference are well in accordance with the results of the present work, as the maximum variation in the results is only of the order of 5.8 %.

5.4 VARIATION OF HARDNESS WITH FLANK-EDGE DISTANCE

The figure 5.2 shows the relation of tool hardness with the flank distance at different temperature distribution on flank edge of the carbide tool bit. As at the tool tip the temperature is maximum, therefore the hardness is less. Using the mathematical model for modified cutting temperature as discussed in section 4.2, the three different values of modified cutting temperatures 750 K, 900 K, and 1050 K, have been calculated from the corresponding strain-rate values which are 840 s^{-1}, 830 s^{-1}, and 577 s^{-1} respectively, corresponding to the different values of feed, speed and depth of cut as shown in table 5.1. At the same flank-edge distance, for these values of modified cutting temperatures, we have different hardness values along the flank face of the tool. The temperature starts decreasing because of heat loss as we move away from the tool tip along the flank surface the hardness of material increases.

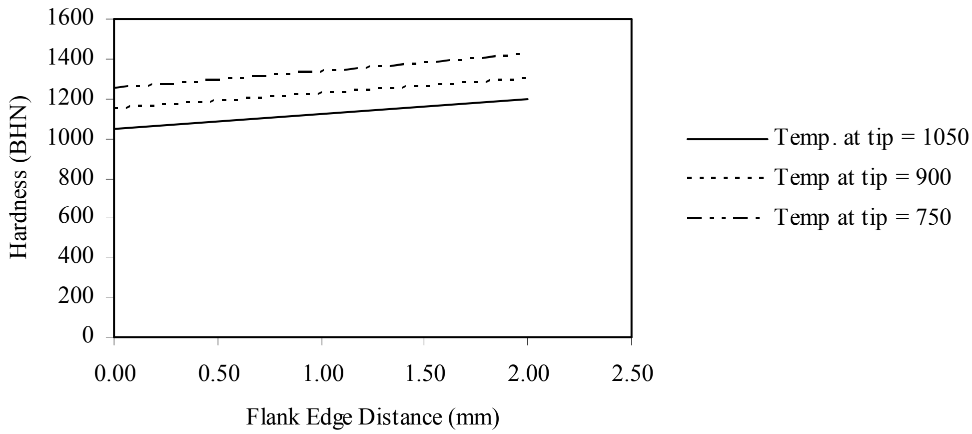

Figure 5.2: Relation between hardness and flank distance

5.5 VARIATION OF TEMPERATURE WITH CUTTING FORCE

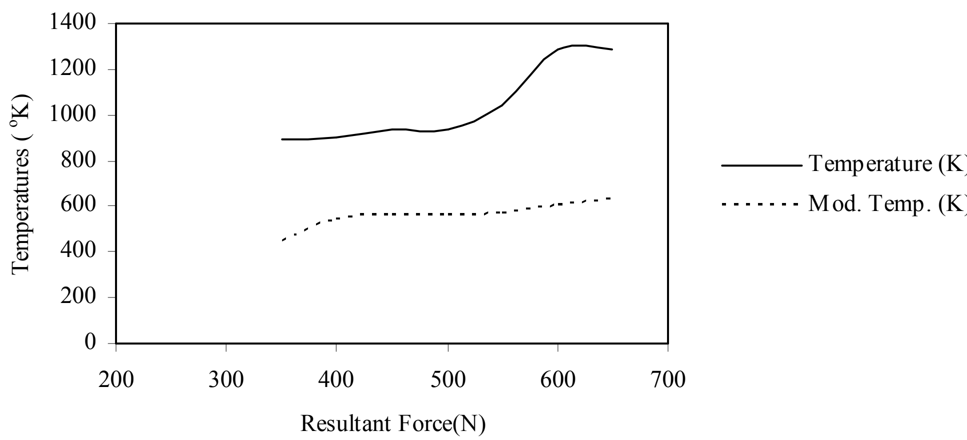

Figure 5.3: Variation of Temperature with resultant cutting force

The figure 5.3 shows the variation of temperature with the cutting force. As shown in the graph, as the cutting forces increases the temperature at the tip of the cutting tool also increases due to higher frictional forces at the tip of the carbide tool bit. This increased temperature of the tool leads to the reduction of hardness value of the cutting tool and thus the tool wear.

5.6 VARIATION OF FLANK WEAR WITH CUTTING FORCE

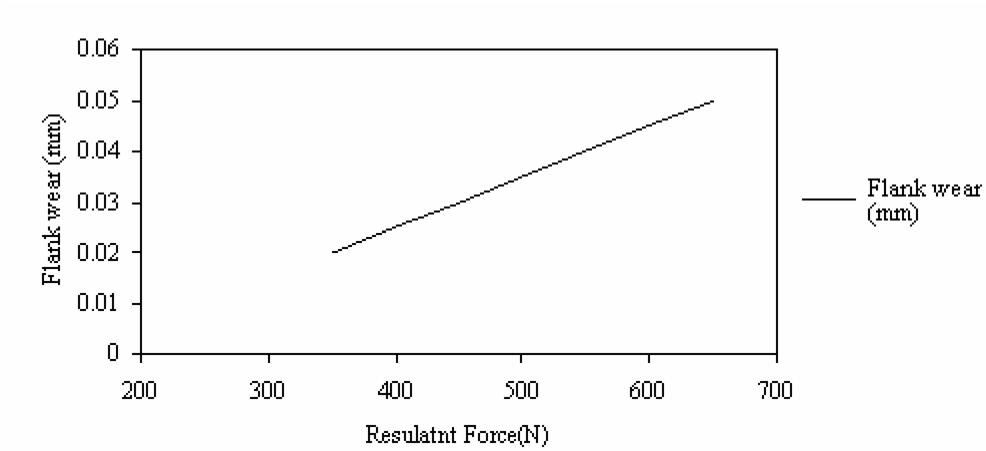

Figure 5.4: Variation of Flank Wear with the resultant cutting force

The figure 5.4 shows the variation of the wear with the cutting tool Force. As shown the flank wear of carbide insert increases with the increase in the forces during the bar turning process. This is because increase in forces leads to increase in the temperature of the cutting tool as shown in figure 5.3 and increased temperatures further leads to the flank wear of the cutting tool due to the thermal softening.

5.7 VARIATION OF FLANK WEAR WITH MODIFIED CUTTING TOOL TEMPERATURE

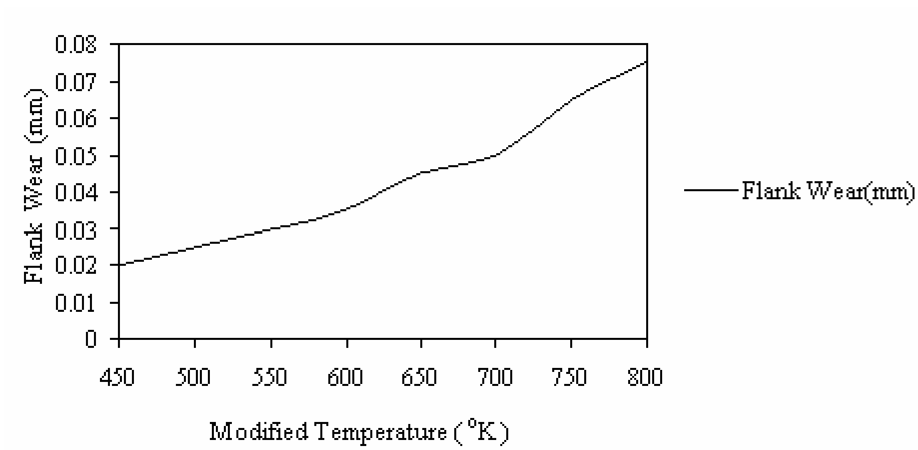

Figure 5.5: Variation of flank Wear with respect to modified temperature

The figure 5.5 shows the variation of the wear with the modified cutting tool temperature due to the strain rate. As shown the flank wear of carbide insert increases with the increase in the temperature of the cutting tool. As increased temperatures at the tip of the cutting tool leads to the reduction of the hardness value, that is the thermal softening, and thus to the flank wear of the carbide cutting tool.

5.8 REGRESSION EQUATION

Regression equations obtained from the experimental data of a bar turning process using carbide insert were obtained using Data Fit software Version8.0.x developed by Oakdale Engineering. The regression equation relating tool flank wear of a carbide insert with cutting parameters (V, f, d) is as follows.

$$\text{Wear (mm)} = e^{(A\times f + B\times d + C\times f + D)}$$

$$A = 1.045,\ B = -6.44 \times e^{15},\ C = 2.015 \times e^{16},\ D = 1.612 \times e^{15}$$

Where v, f and d are levels of cutting speed (v), feed (f) and depth of cut (d) respectively and values for these levels can be obtained by following Formula:

$$\text{Level} = \frac{(\text{actual value in the range - mean value of the range})}{(\text{Difference Between maximum and middle level})}$$

5.9 VARIATION OF TEMPERATURE WITH CUTTING VELOCITY

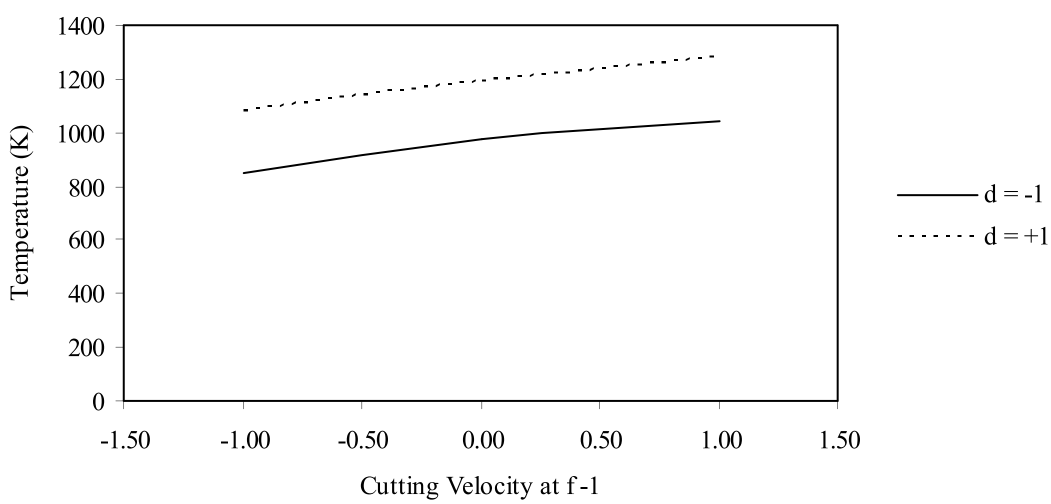

Figure 5. 6: Relation between Cutting velocity and temperature at feed rate (f = -1)

The figure 5.6 shows a relation of cutting velocity versus temperature, at constant feed at different levels depth of cuts used in experimentation work. The inference that can be drawn from the above graph is that when we increase the cutting velocity the temperature keeps on increasing.

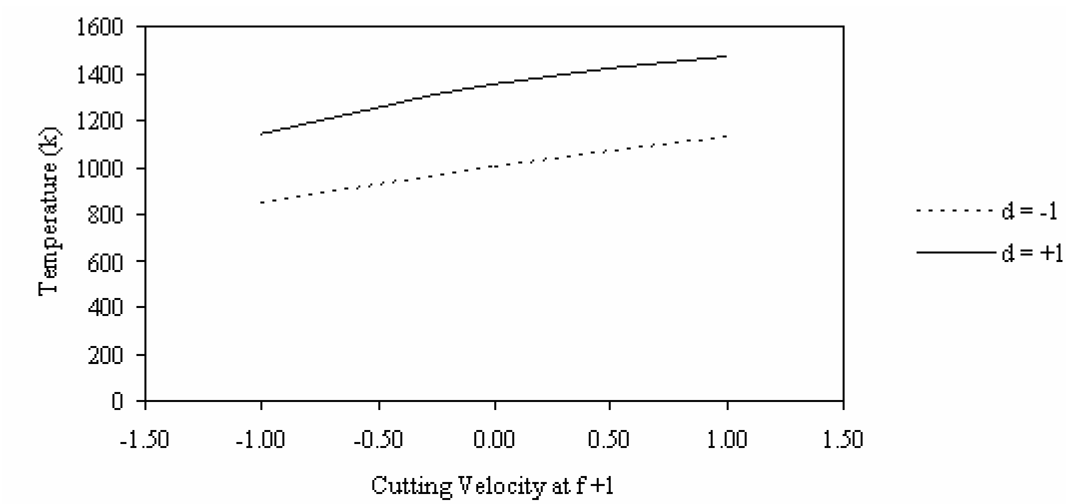

Figure 5.7: Relation between Cutting velocity and temperature at feed rate (f = +1)

The figure 5.7 depicts the same trends as figure 5.6, from these trends it's depicted that with the increase in velocity of cutting, the temperature raises. These two graphs are at constant depth of cuts for each curve. The figure 5.8 shows results of temperature with cutting velocity at constant depth of cuts. It shows temperature increase with increase in depth of cut.

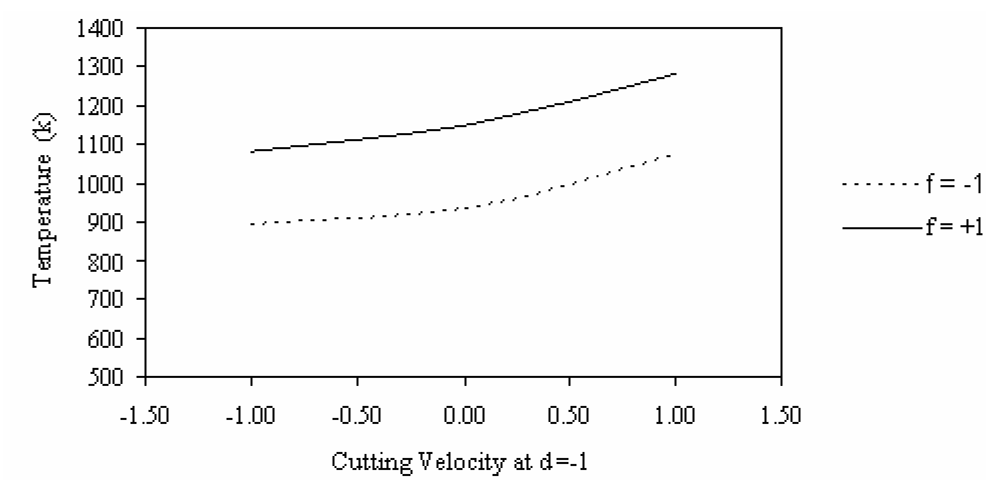

Figure 5.8: Variation of Temperature versus cutting velocity at depth of cut (d = -1)

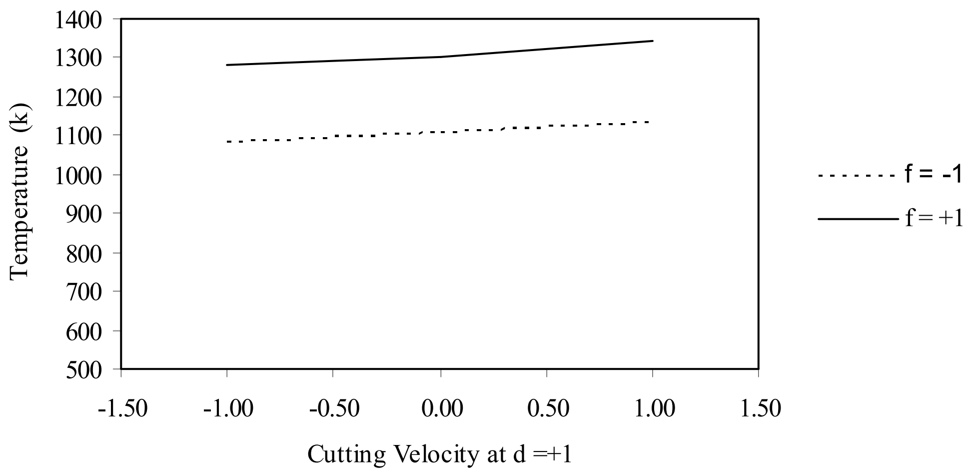

Figure 5.9: Variation of Temperature versus cutting velocity at depth of cut (d = +1)

Similarly figure 5.9 shows the graph but at different machining parameters and conditions (d = +1). The trend line is depicted to be same as it increases with rise in velocity of cutting.

5.10 VARIATION OF FLANK WEAR WITH CUTTING VELOCITY (FOR CONSTANT FEED RATE)

Figure 5.10: Variation of flank wear with cutting velocity at constant feed rate (f = -1)

Here the results have been shown for the variation of wear with the cutting velocity of the tool. In figure 5.10 trend of cutting velocity with wear has been shown at constant feed of -1, that is the lowest feed taken in experiments at different depth of cuts shows almost same pattern of increasing flank wear with increase in velocity. The figure 5.11 depicts same trends of wear but here now feed rate is (f = +1). The results seem almost similar for this case too.

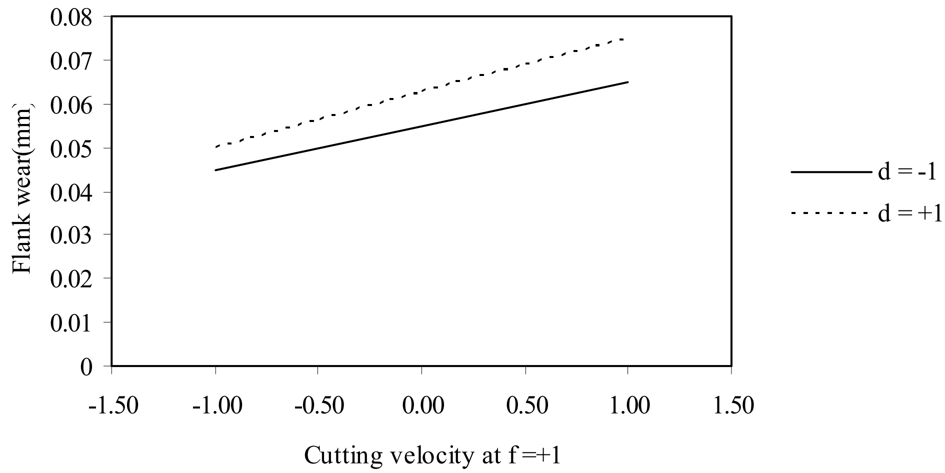

Figure 5.11: Variation of flank wear with cutting velocity at constant feed rate (f= +1)

5.11 VARIATION OF FLANK WEAR WITH CUTTING VELOCITY (FOR CONSTANT DEPTH OF CUTS)

The graphs discussed till now were at constant feed rate, for better understanding of wear trends graphs are also shown at constant depth of cuts. The figure 5.12 shows results of wear with cutting velocity at constant depth of cuts.

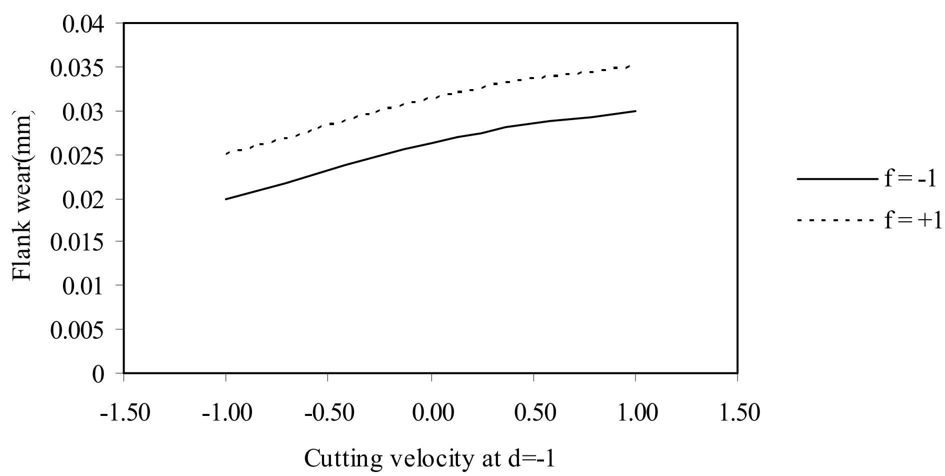

Figure 5.12: Variation of flank wear with cutting velocity at constant depth of cut (d = -1)

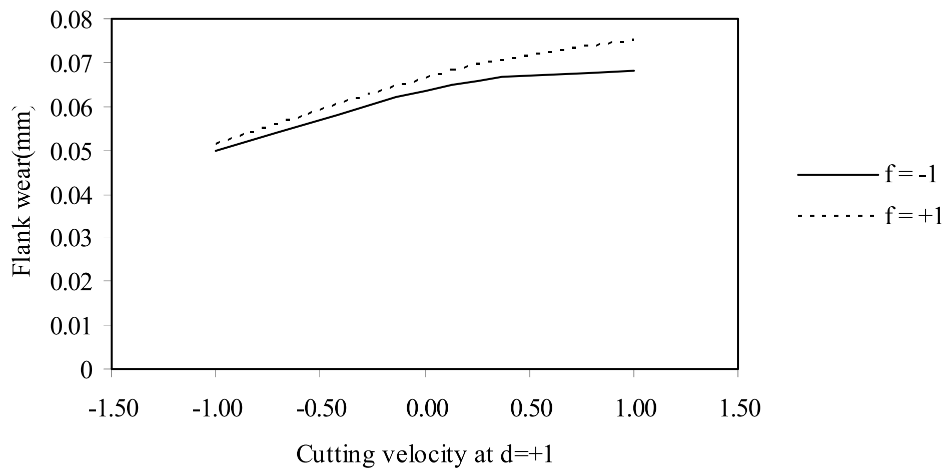

Figure 5.13: Variation of flank wear with cutting velocity at constant depth of cut (d =+1)

The figure 5.13 also shows similar results but at depth of cuts (d = +1). The trend is almost same depicted in other graphs as shown before, that is with increase in the cutting velocity for some constant value of depth of cut, the tool wear increases.

5.12 CONCLUSIONS

Based on the results presented in previous sections, the following conclusions have been observed:

1. The hardness increases with increase in distance from the flank edge and with decrease in the tool-workpiece contact temperature.
2. The change in the tool workpiece contact temperature depends upon the cutting parameters and it increases with increase in resultant cutting force, but do not follow a linear trend and thus we can find an optimum set of machining parameters to have a minimum heat generation at tool-workpiece contact.
3. The flank wear is directly proportional to the resultant cutting force and approximately follows a linear trend.
4. The flank wear increases with increase in modified cutting tool temperature (due to increase in the strain rate), but there is a nonlinear trend so we can find an optimum value of cutting parameters so as to give minimum strain rate, because heat generated increases with increase in the strain rate.
5. The contact temperature increases with the increase in the cutting velocity, but at constant cutting velocity, there is a significant increase in the contact temperature with

increase in the depth of cut as compared to the increase in the contact temperature with the increase in the feed rate.

6. The flank wear increases significantly with the increase in the cutting velocity. Also at constant cutting speed it increases with increase in both feed rate and depth of cut.

Thus finally it can be observed that we must select the cutting parameters, which are cutting speed, feed rate, and depth of cut, in such a way so as to have the optimum temperature at the tool tip-workpiece contact because of the heat generated, so that the minimum tool wear is encountered, and thus we could have the longest tool life and better machining economy.

5.13 SCOPE FOR FURTHER WORK

With increasing competitiveness as observed in the recent times, manufacturing systems in the industry are being driven more and more aggressively. So there is always need for perpetual improvements. Thus for getting still more accurate results we can take into account few more parameters as given below:

- The transient analysis for the machining operation can be studied.
- The study can also be extended on coated carbide tools, CBN, or other harder tools.
- CNC machines can be used for the experimentation to have the better control of the process variables and also parameters can be set to the desired accuracy.
- The presently developed system can be used for other conventional as well as unconventional processes such as milling, drilling.
- The other combinations of machine, cutting tool and work material can be studied.

APPENDIX - A

SPECIFICATIONS OF THE CENTRE LATHE

Center Height	200 mm
Center Distance	1000 mm
Swing	
Over Bed	420 mm dia
Over Cross slide	220 mm dia
In Gap	550 mm dia
Gap Width	155 mm dia
Transverse	
Of Cross slide	225 mm
Of Top	125 mm
Of Tailstock Spindle	150 mm
Spindle Bore	53 mm dia
Spindle Bore Taper	Metric Short No. 7
Spindle Speed	32-1200 rpm
Spindle Speed Ratio	1.69
Tool Shank Size	25x25, 20x20 mm
Feed	
Longitudinal Feeds	0.05-2.7 mm/rev
Cross Feed	0.01-0.54 mm/rev
Main Motor	2.2KW/3 HP
Weight of Machine	1250 Kg
Height of the Spindle Center above Floor	1035 mm
Floor Space	915x2725 mm
3 Phases, 415 V, 50 Hz, AC Supply	

APPENDIX –B
WORKPIECE SPECIFICATIONS

• Work piece material	:	EN 24steel
• Work piece combination	:	0.35- 0.45 %C
		0.45- 0.6 %Mn
		1.3 - 1.8 %Ni
		0.9 - 1.4 % Co
		0.2 - 0.3 % Cr
		0.1 - 0.35% Si
		And rest is Iron
• Work piece hardness	:	260BHN
• Cutting tool material	:	K10 CARBIDE INSERT
• Hardness	:	1500 BHN

APPENDIX – C
WORKPIECE SPECIFICATIONS

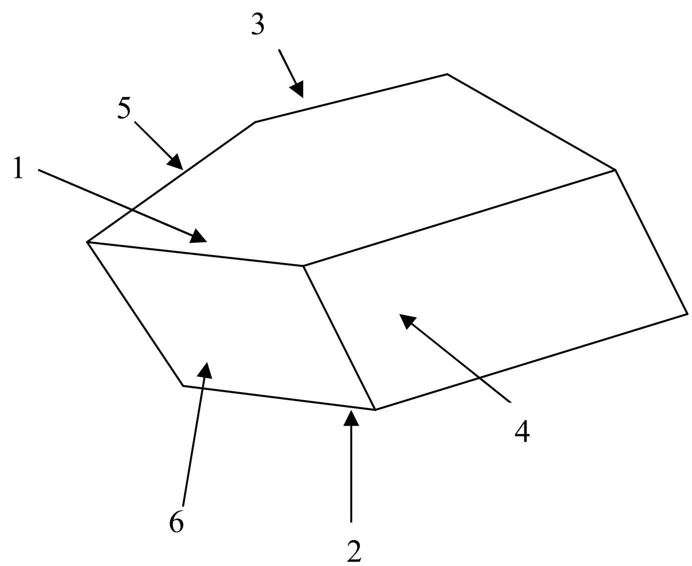

Figure A-C.1: Convection faces used in FEM analysis of Carbide cutting tool

Here 1, 2, 3, 4, 5, 6 are the faces through which the heat is lost to the environment (convection heat loss).

Books

[1] J N Reddy, “An introduction to finite element Method”, McGraw-Hill, 1993.

[2] B.S Raghuwanshi, “A Course in Workshop Technology”, Dhanpat Rai & Co, Vol-2 (1998).

[3] G.K.Lal, “Introduction to machining science”, New Age International Publishers, 1999.

[4] R.K.Jain, “Production Technology”, Khanna Publishers, 2001

[5] Tirupathi R.Chandrupatla, Ashok D. Belegundu, “Introduction to Finite Elements in Engineering”, Pearson Education, 2002.

Research Papers

[1] Shih Albert J., Yang Henry T.Y., “Experimental and Finite Element Predictions of Residual Stresses due to Orthogonal Metal Cutting”, International Journal for Numerical Methods in Engineering, vol. 36(1993), pp.1487-1507.

[2] Shih Albert J, “Finite Element Simulation of Orthogonal Metal Cutting”, Journal of Engineering for Industry”, ASME, vol. 117(1995), pp. 84-93.

[3] Gillibrand D., Bradbury S.R., Yazdanpanah, Mobayyen S.,“A Simplified approach to Evaluate the Thermal Behaviour of Surface Engineered Cutting Tools”, Journal of Surface & Coatings Technology, vol. 82(1996), pp.344- 351.

[4] Leshock C.E., Shin Y.C., “Investigation on cutting Temperature in Turning by a Tool-Work thermocouple technique”, Journal of Manufacturing Science and Engineering, vol. 119 (1997), pp. 502 – 508.

[5] Mills B., Hao C.S., Qi H.S., “Formation of an adherent layer on a cutting tool studied by micro machining and finite element analysis”, Wear, vol. 208(1997), pp. 61-66.

[6] Tieu A.K., Fang X.D., Zhang D., “FE analysis of cutting tool temperature field with adhering layer formation”, Wear, vol. 214 (1998), pp. 252-258.

[7] Chu T.H., Wallbank J., “Determination of the temperature of a machined surface”, Journal of Manufacturing Science and Engineering, vol.120 (1998), pp. 259-263.

[8] Ostafiev V., Kharkevich A.,Weinert K.,Ostafiev S., "Tool Heat Transfer in Orthogonal Metal Cutting", Journal of Manufacturing Science and Engineering, vol. 121(1999),pp. 541-549.

[9] Chou Kevin Y., Evans J.Chris, "White layers and thermal modeling of hard turned surfaces", International Journal of Machine Tools & Manufacture, vol. 39 (1999), pp. 1863–1881.

[10] Choudhury S.K., Kishore K.K., "Tool Wear Measurement in Turning using Force Ratio", International Journal of Machine Tools and Manufacture, vol.40(2000), pp. 899-909.

[11] Lim C.Y.H., Lau P.P.T., Lim S.C., "The effects of work material on tool wear", Wear, vol. 250(2001),pp. 344–348.

[12] Sullivan D.O., Cotterell M., "Temperature measurement in single point turning", Journal of Material Processing Technology, vol. 118(2001), pp. 301-308.

[13] Komanduri R., Hou Z.B., et al, "Tribology in Metal Cutting-Some Thermal issues", Journal of Tribology, vol.123 (2001), pp. 799 - 815.

[14] Huda Mahfudz Al, Yamada Keiji, Hosokawa Akira, Ueda Takashi, "Investigation of Temperature at Tool-Chip Interface in Turning Using Two-Color Pyrometer", Journal of Manufacturing Science and Engineering, vol. 124(2002),pp. 200-207.

[15] Yen Y.C.,Sohner J.,Weule H.,Schmidt J.,Altan T., "Estimation of tool wear of carbide tool in orthogonal cutting using Fem simulation", Machining Science & Technology, vol. 6(2002) ,pp. 467-486.

[16] Strenkowski J.S., Shih A.J., Lin J.C., "An analytical finite element model for predicting three-dimensional tool forces and chip flow", International Journal of Machine Tools & Manufacture ,vol. 42 (2002),pp. 723–731.

[17] Chiou Richard Y., Chen Jim S J., Lu Lin, and Cole Ian, "Prediction of heat transfer behavior of carbide inserts with embedded heat pipes for dry machining", Proceedings of ASME 2002.

[18] Zhao H., Barber G.C., Zou Q., "A study of flank wear in orthogonal cutting with internal cooling", Wear, vol. 253 (2002),pp. 957–962.

[19] Yen Yung-Chang, Sohner Jorg, Lilly Blaine, Altan Taylan, "Estimation of tool wear in orthogonal cutting using the finite element analysis", Journal of Material Processing Technology (2003) (R&D Update Machining 2002).

[20] Amir H. Adibi-Sedeh, Vis Madhavan, Behnam Bahr, "Extension of Oxley's Analysis of Machining to Use Different Material Models", Transactions of the ASME ,vol. 125 (2003) ,pp. 656-666.

[21] Miller Mark R., Mulholland George, Anderson Charles, "Experimental Cutting Tool Temperature Distributions", Journal of Manufacturing Science and Engineering, vol. 125(2003), pp. 667-673.

[22] Arsecularatne J.A., Kristyanto B.,and Mathew P., "An Investigation of the high speed machining process using a variable flow stress machining theory", Machining Science and Technology ,vol.8 (2004) ,pp. 211-233.

[23] Ranc N., Pina V., Sutter G., Philippon S., "Temperature Measurement by Visible Pyrometry: Orthogonal Cutting Application", Journal of Heat Transfer, vol. 126 (2004), pp. 931-936.

[24] Sinha Aman, "Condition monitoring of tool and workpiece in turning using neural network", M Tech thesis, Department of Mechanical Engg. TIET, Patiala, India 2004.

[25] Chou Kevin Y., Song Hui, "Thermal modeling for white layer predictions in finish hard turning", International Journal of Machine Tools & Manufacture (2004), pp.1–15 (Article in Press).

[26] Moufki A., Devillez A., Dudzinski D., Molinari A., "Thermo mechanical modeling of oblique cutting and experimental validation", International Journal of Machine Tools & Manufacture, vol. 44 (2004), pp. 971–989.

[27] Molinari A., Moufki A., "A new thermo mechanical model of cutting applied to turning operations, Part I- Theory", International Journal of Machine Tools & Manufacture, vol. 45(2005), pp. 166–180.

[28] CAKIR Cemal M., ISIK Yahya., "Finite element analysis of cutting tools prior to fracture in hard turning operations", Journal of Materials and Design, vol. 26 (2005), pp. 105–112.

[29] Sharma Gagnesh, "Analysis of a Carbide Insert for Flank Wear monitoring during

Turning using Finite Element Method", M Tech thesis, Department of Mechanical Engg. TIET, Patiala, India 2004.